SUPPORTING INFORMATION

Modulation of specialized metabolite production in genetically engineered *Streptomyces pactum*

Zhiran Ju, Wei Zhou, Hattan A. Alharbi, Daniel C. Howell and Taifo Mahmud*

Department of Pharmaceutical Sciences, Oregon State University, Corvallis, OR 97331-3507 (USA)

Corresponding author: Taifo Mahmud. E-mail: Taifo.Mahmud@oregonstate.edu; Fax: (+1) 541-737-3999; Address: Oregon State University College of Pharmacy, 203 Pharmacy Building, Corvallis, OR 97331, USA.

T. Mahmud's ORCID ID: 0000-0001-9639-526X

Supplementary Methods

General Experimental Procedures. Optical rotations were measured using a Jasco P1010 polarimeter. UV spectra were recorded on an Eppendorf BioSpectrometer. The NMR spectra were measured on a Bruker Avance III 700 MHz NMR spectrometer equipped with a 5 mm ^{13}C cryogenic probe. Low-resolution mass spectra were obtained from an AB SCIEX 3200 QTRAP mass spectrometer and high-resolution ESI mass spectra were obtained using an Agilent 1260 HPLC upstream of an Agilent 6545 Q-ToF. Semi-preparative reversed-phase HPLC was performed on an Agilent 1260 Infinity II series apparatus.

Construction of *S pactum* Mutants. Gene disruptions were performed according to the general protocols reported in our previous papers.[1, 2] In brief, the upstream and downstream homologous arms of the deleted sequence were amplified from the genome of *S. pactum* using primers described in Supplementary Table 3, and the products were cloned into the plasmid pTMN002 at the XbaI and HindIII sites. The plasmids (pTMN002-nftCD, pTMN002-congC1-C2, pTMN002-BGC2.4, and pTMN002-BGC1.26) (Supplementary Table 4) were individually transferred into *S. pactum* by conjugation with *E. coli* ET12567/pUZ8002. The single crossover mutants were selected on BTT agar plates containing apramycin 50 $\mu g\ mL^{-1}$. The second crossover mutants were selected by replica plating on BTT agar plates with and without apramycin. The mutants were verified by PCR analysis. The information of primers and plasmids used for gene disruption were summarized in Supplementary Tables 3 and 4.

In Vitro Anti-bacterial Test of Conglobatins. Test bacteria (*S. aureus*, *B. subtilis*, *P. aeruginosa* and *E. coli*) were grown on agar plates (LB) for 1-2 days at 37 °C and then added to liquid LB medium. After shaking at 200 rpm, 30 °C, for 5 to 20 h, the cultures were diluted with LB medium to obtain an OD_{600} value of 0.1. Bacterial cultures (100 μL) with the desired optical density value were added to LB medium (50 mL) and then mixed gently. The bacterium-containing medium (98 μL) were then added to each well of 96-well plates containing DMSO solutions (2 μL) of the tested compounds at different concentrations. DMSO was used as a negative control and ampicillin was used as a positive control. The 96-well plates were placed in an incubator for 17 to 48 h. An MTT solution (50 μL, 1 mg mL^{-1}) was then added to each well. After letting them stand for 30 min, the color change was observed. All experiments were performed in triplicate. The minimum inhibitory concentration values were determined as the lowest concentration required for bacterial growth inhibition.

In Vitro Cytotoxicity Test of Conglobatins. HeLa, MCF-7, NCI-H460, and RAW264.7 cancer cell lines were obtained from the American Type Culture Collection (ATCC). Cells were cultured at 37 °C in a 5% CO_2 humidified incubator and maintained in high glucose Dulbecco's Modified Eagle Medium (DMEM, Nissui) containing 100 mg mL^{-1} streptomycin, 2.5 mg L^{-1} amphotericin B, and 10% heat-inactivated fetal bovine serum (FBS). Suspensions of tested cell lines (calc. 1.0×10^4 cells/well) were seeded in 96-well culture plates and cultured for 12 h followed by treatment with various diluted concentrations of test compounds for 48 h. Control cultures were treated with culture medium alone. The tested compounds were evaluated at six dilutions and the highest concentration was 50 μM. Cell viabilities were evaluated using the MTT assay, which was

added to each well (20 µL, 5 mg mL^{-1}) and incubated at 37 °C for 4 h in the dark. After adding DMSO (150 µL) to dissolve the formed insoluble formazan crystals, absorbance was read using a SpectraMax 190 Reader (Molecular Devices) at a wavelength of 490 nm. Cells in the exponential phase were used for all experiments.

Molecular Modeling. Docking calculations were performed using Auto Dock Vina 1.1.2 software. The default settings and scoring function of Vina were applied. The AMBER force field was applied for energy minimization. For ligand preparation, Chem3D Ultra 8.0 software was used to convert the 2D structures of the candidates into 3D structural data and to prepare the chemical structures with minimized energy. Protein coordinates were downloaded from the Protein Data Bank. Chain A was prepared for docking within the molecular modeling software package Chimera 1.5.3 by removing co-chaperone Cdc37, all ligands and water molecules, and by calculating the protonation state of the protein. Addition of polar hydrogen and setting of grid box parameters was performed using MGLTools 1.5.4. PyMol v1.5 was used to analyze and visually investigate the ligand-protein interactions of the docking poses.

Supplementary Tables

Supplementary Table 1. In vitro cytotoxicity test of the conglobatins against cancer cell lines.

Compound	IC_{50} (μM)			
	HeLa	NCI-H460	MCF-7	RAW264.7
Conglobatin	7.05	13.38	32.26	83.29
Conglobatin B2	14.25	13.37	32.0	> 100
Conglobatin B3	11.68	79.72	39.68	> 100
Conglobatin F1	14.97	26.37	> 100	> 100
Conglobatin F2	3.72	7.43	27.24	> 100

Supplementary Table 2. Calculated binding affinity values of conglobatin and its derivatives

Compound	Affinity Value (Kcal/mol)
Conglobatin	-8.1
Conglobatin B1	-7.2
Conglobatin B2	-7.9
Conglobatin B3	-8.0
Conglobatin F1	-7.8
Conglobatin F2	-8.0

Supplementary Table 3. Primers used in this study

Primers	Sequence (5′→3′)	Source
spcongC-UF(XbaI)	AGCTCTAGAGACAGGGAAGACGCCATTGCGGAG	[3]
spcongC-UR(BamHI)	ACGGGATCCCTCTGCCAGGTCCTCCCGTTCGAC	[3]
spcongC-DF(BamHI)	ACGGGATCCTGGGCTCGCTGAAGTCCAACATCG	[3]
spcongC-DR(HindIII)	AGGAATTCGCCGTGCAGCAGGGGCACGAAGG	[3]
T-spcongC-F	GTGTAGAGGGCGATCTCG	[3]
T-spcongC-R	TCCTCGTTCGGCGTCAGC	[3]
BGC2.4-UF(XbaI)	AGCTCTAGAACCGCGTTCGTGATGTTCTCCTCCTC	This study
BGC2.4-UR(BamHI)	ACGGGATCCGTCGGAGAGCTTCTCCAGCAGCAGG	This study
BGC2.4-DF(BamHI)	ACGGGATCCGACCACGTGGTGCTCGGCACCGTCG	This study
BGC2.4-DR(HindIII)	ACCCAAGCTTCGAGGGCGTCCAGGAACAGGTTGG	This study
BGC1.26-UF(XbaI)	AAGCTCTAGATCTTCGTCCGCAGGCTGCT	This study
BGC1.26-UR(BamHI)	AACGGGATCCGAACTCCGAGATCGCGTCG	This study
BGC1.26-DF(BamHI)	AACGGGATCCATCATCGAACAGGCCCCGACC	This study
BGC1.26-DR(HindIII)	AACCCAAGCTTGTCGCCGGTGAGGTTGGAGA	This study
PieA5-seguence-F	ACAAACTGGAGGCGGTGCTCGAC	This study
PieA5-sequence-R	TAGCCGAAGACGTGGTCGACGTC	This study
PieA6-sequence-F	AGCAAGGACCTGTTCGATGCGTAC	This study
PieA6-sequence-R	GACCTGGAGAGCCTGTACGA	This study

Supplementary Table 4. Plasmids and strains used in this study

Plasmids	Description	Reference
pTMN002	pJTU1278+ derivative containing an OriT transfer element and 101 ori	[1]
pTMN002-nftCD	Plasmid pTMN002 carrying upstream and downstream homologous arms of *nftCD*	[4]
pTMN002-congC1-C2	Plasmid pTMN002 carrying upstream and downstream homologous arms of *spcongC1* and *spcongC2*	[3]
pTMN002-BGC2.4	Plasmid pTMN002 carrying upstream and downstream homologous arms of *pieA5*	This study
pTMN002-BGC1.26	Plasmid pTMN002 carrying upstream and downstream homologous arms of *pieA6*	This study
Strains		
S. pactum WT	*S. pactum* ATCC 27456 wild type	ATCC
S. pactum Δ*ptmTDQ*	*S. pactum* ATCC 27456 with the *ptmT*, *ptmD* and *ptmQ* genes deleted, which cannot produce pactamycin	[4]
S.pactum Δ*ptmTDQ*/ΔBGC-1.2	*S. pactum* Δ*ptmTDQ* with the *nftC* and *nftD* genes inactivated by in-frame deletion	[4]
S.pactum Δ*ptmTDQ*/ΔBGC-1.2/ΔBGC-1.23	*S. pactum* Δ*ptmTDQ*/ΔBGC1.2 with the *spcongC1* and *spcongC2* genes inactivated by in-frame deletion	This study
S.pactum Δ*ptmTDQ*/ΔBGC-1.2/ΔBGC-2.4	*S. pactum* Δ*ptmTDQ*/ΔBGC1.2 with the *pieA5* gene inactivated by in-frame deletion	This study
S.pactum Δ*ptmTDQ*/ΔBGC-1.2/ΔBGC-1.26	*S. pactum* Δ*ptmTDQ*/ΔBGC1.2 with the *pieA6* gene inactivated by in-frame deletion	This study

Supplementary Figures

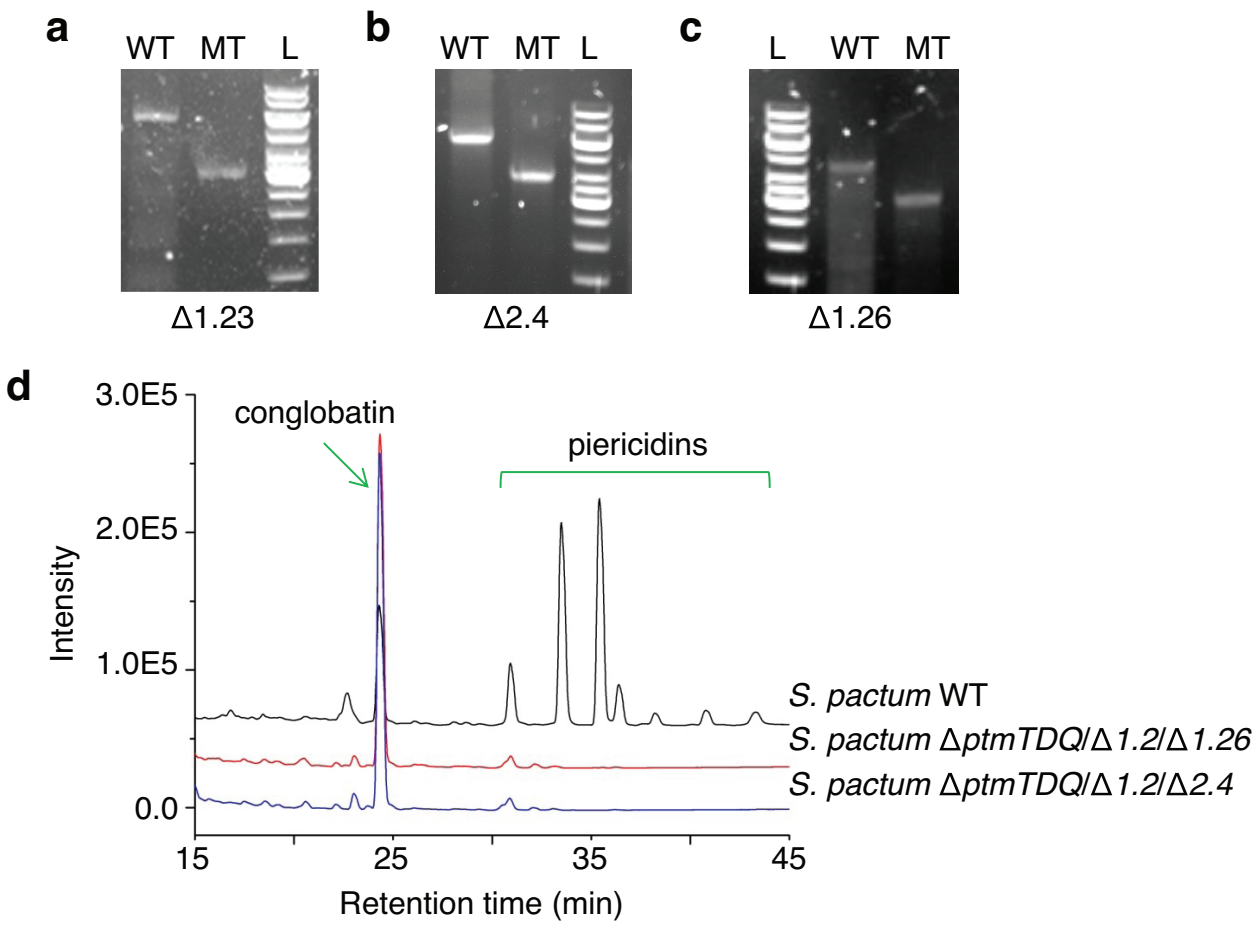

Supplementary Figure 1. Gel electrophoresis of PCR fragments from and metabolic profiles of *S. pactum* mutants. (**a**) *S. pactum* Δp*tmTDQ* mutant (labeled as WT) and *S. pactum* Δ*ptmTDQ*/Δ1.2/Δ1.23 mutant (labeled as MT); (**b**) *S. pactum* Δp*tmTDQ* mutant (labeled as WT) and *S. pactum* Δ*ptmTDQ*/Δ1.2/Δ2.4 mutant (labeled as MT); (**c**) *S. pactum* Δp*tmTDQ* mutant (labeled as WT) and *S. pactum* Δ*ptmTDQ*/Δ1.2/Δ1.26 mutant (labeled as MT). L is DNA ladder; (**d**) HPLC chromatograms of *S. pactum* wild-type, *S. pactum* Δ*ptmTDQ*/Δ1.2/Δ1.26, and *S. pactum* Δ*ptmTDQ*/Δ1.2/Δ2.4.

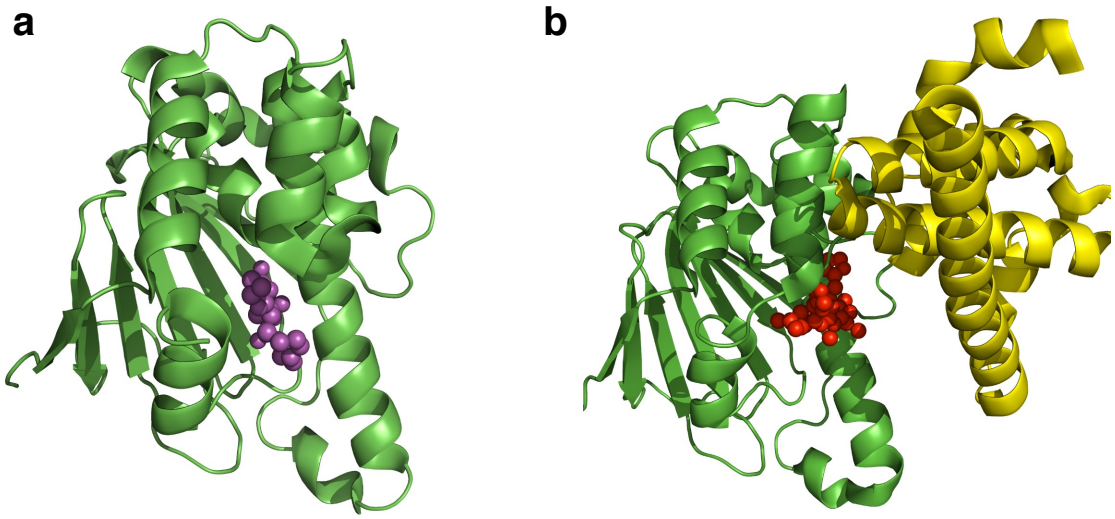

Supplementary Figure 2. Docking structures of ligand/Hsp90 binding. (**a**) Geldanamycin (GA) binds to N-terminal Hsp90 in the ATP binding pocket. Hsp90 is shown in the green ribbon view; GA is shown in purple ball view. (**b**) Conglobatin binds to the N-Hsp90/Cdc37 complex. N-Hsp90 is shown in green ribbon view; Cdc37 is shown in yellow ribbon view; conglobatin is shown in red ball view (Protein Data Bank [PDB] ID: 2K5B)).

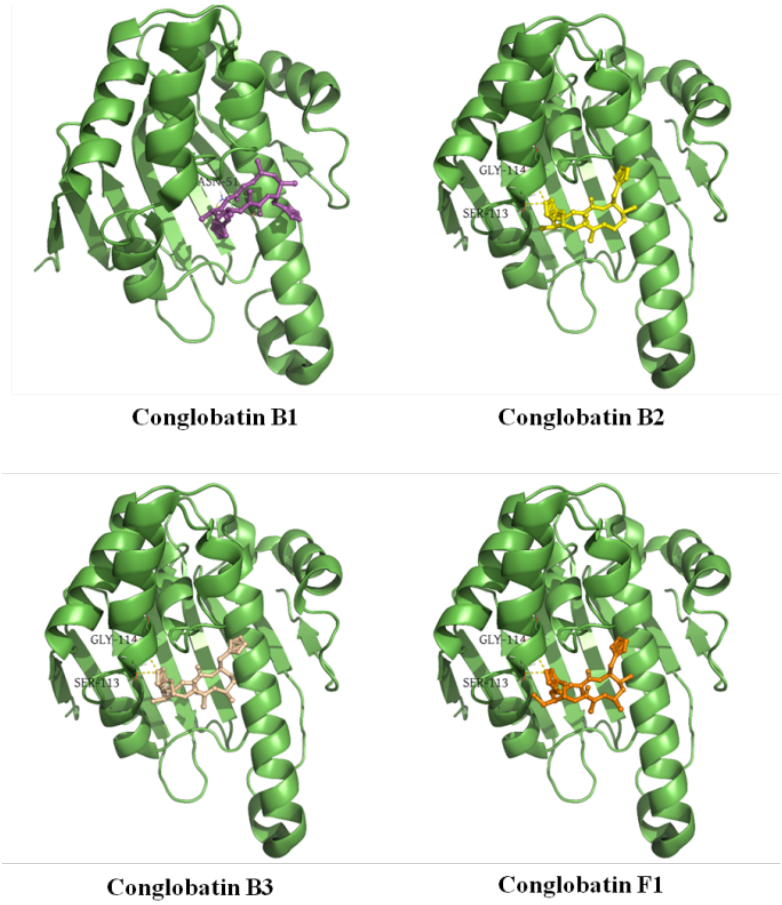

Supplementary Figure 3. Docking structures of ligand/Hsp90 binding. Hsp90 is shown in the green ribbon view; conglobatins B1, B2, B3, and F1 are shown in different color stick view (Protein Data Bank [PDB] ID: 2K5B).

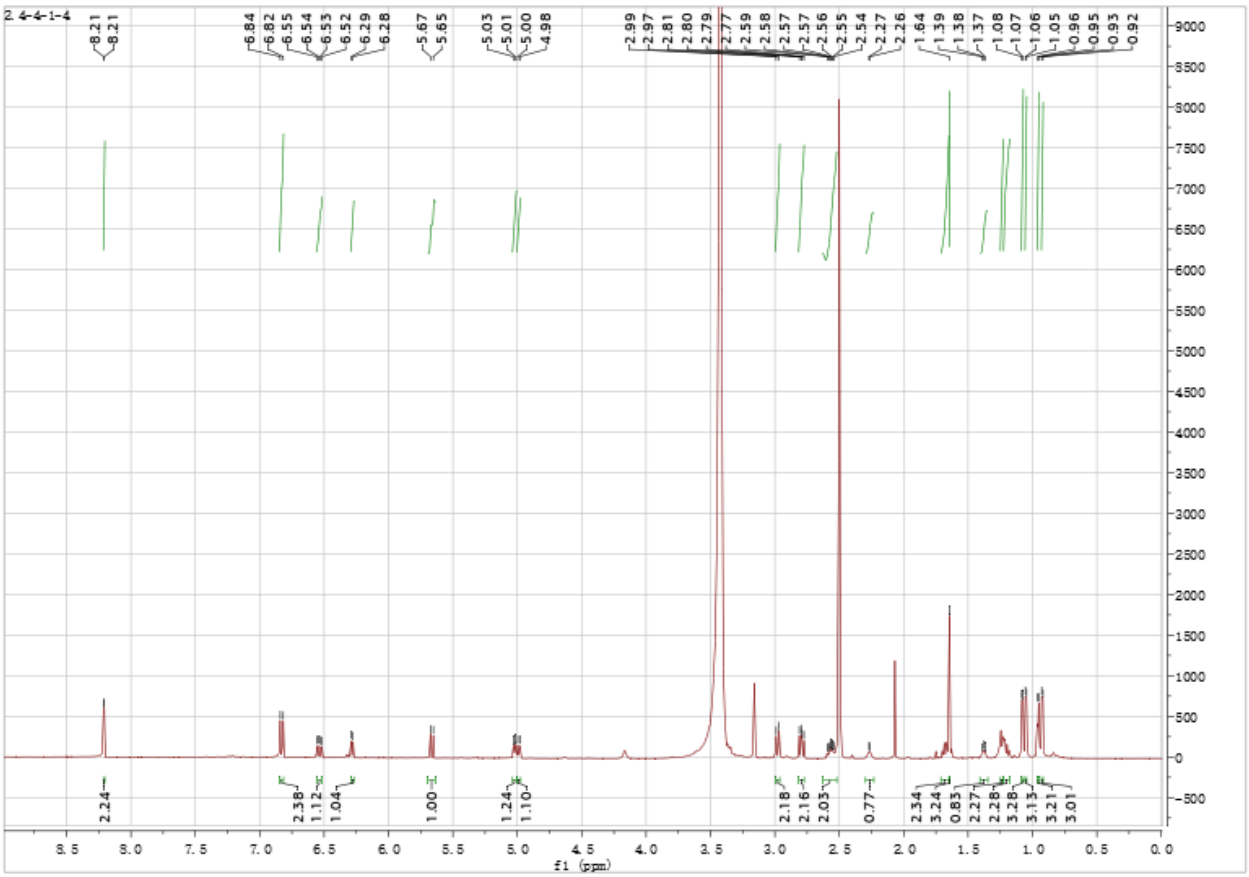

Supplementary Figure 4. ^{1}H NMR spectrum of conglobatin B2 (700 MHz in DMSO-d6).

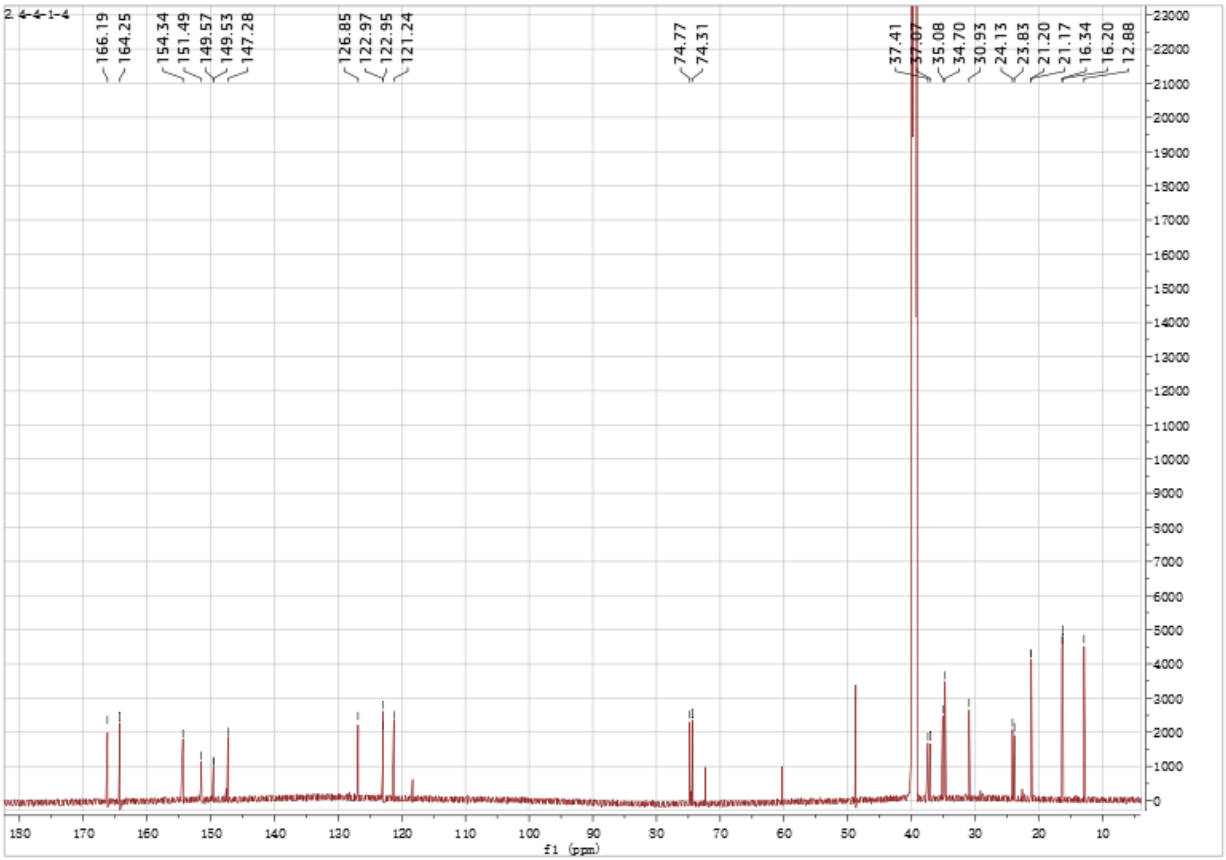

Supplementary Figure 5. ^{13}C NMR spectrum of conglobatin B2 (175 MHz in DMSO-d6).

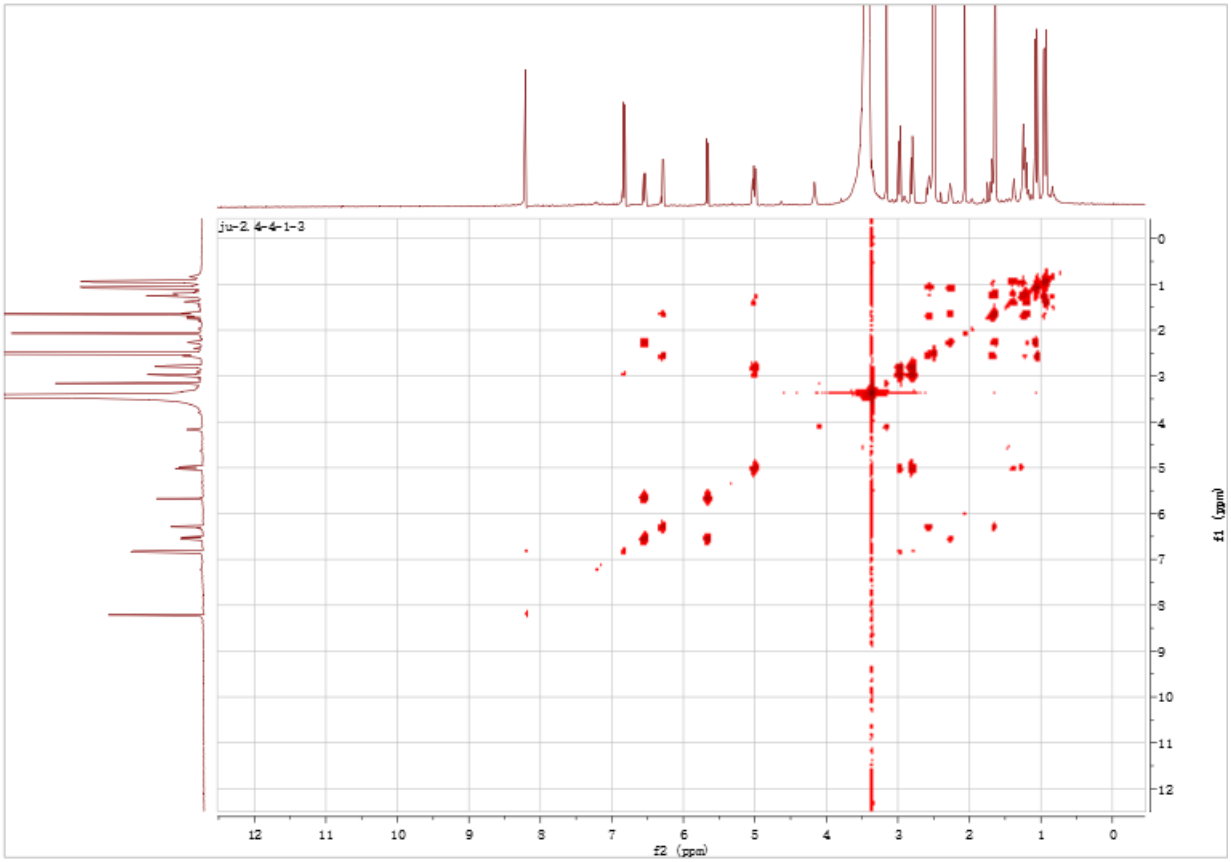

Supplementary Figure 6. ^{1}H-^{1}H COSY spectrum of conglobatin B2 (700 MHz in DMSO-d6).

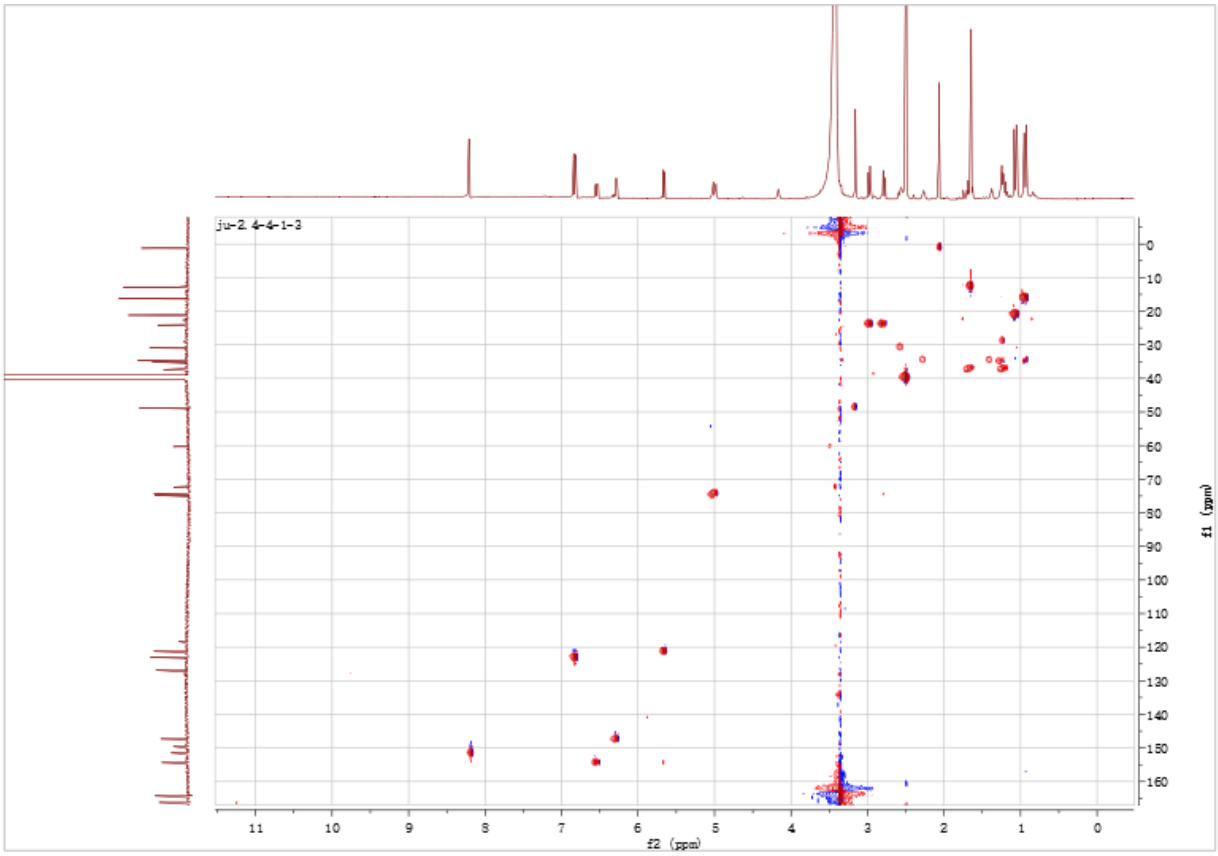

Supplementary Figure 7. HSQC spectrum of conglobatin B2 (700 MHz in DMSO-d6).

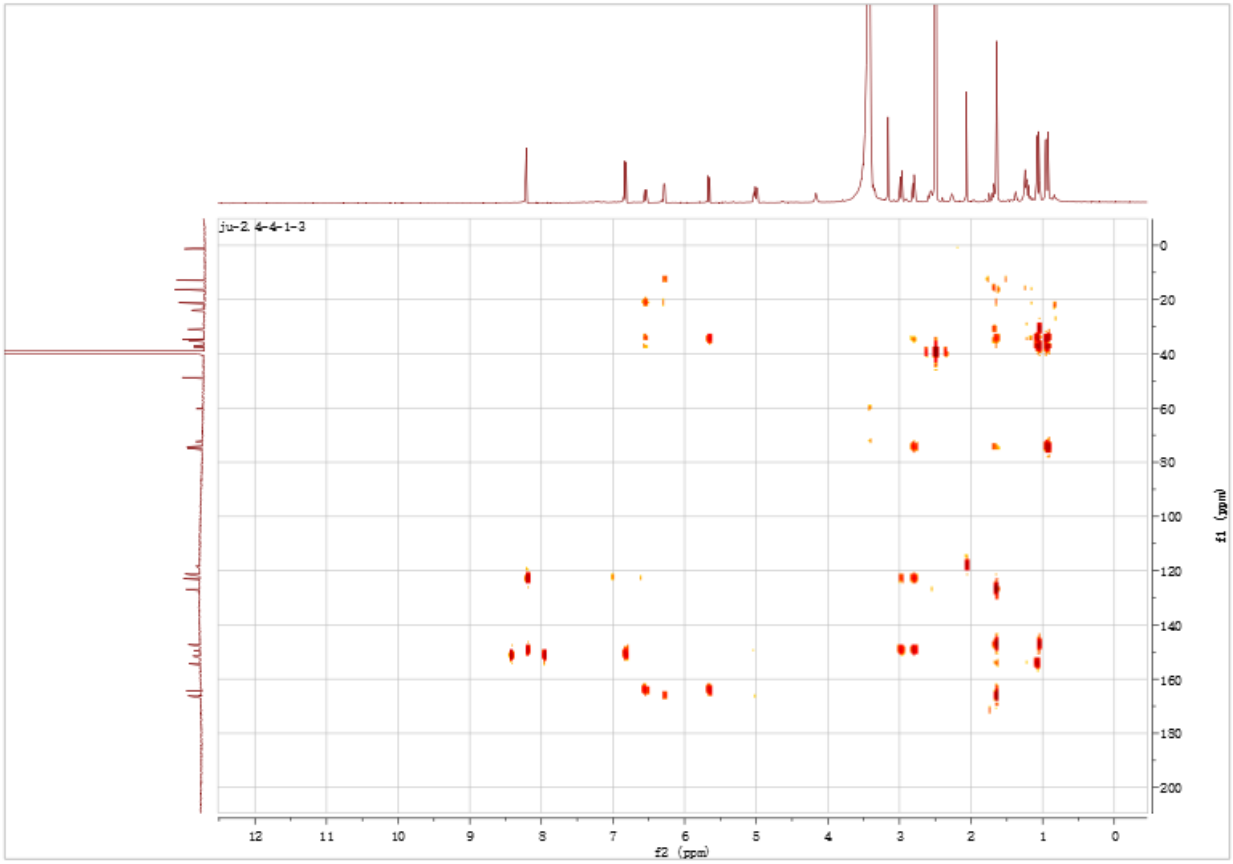

Supplementary Figure 8. HMBC spectrum of conglobatin B2 (700 MHz in DMSO-d6).

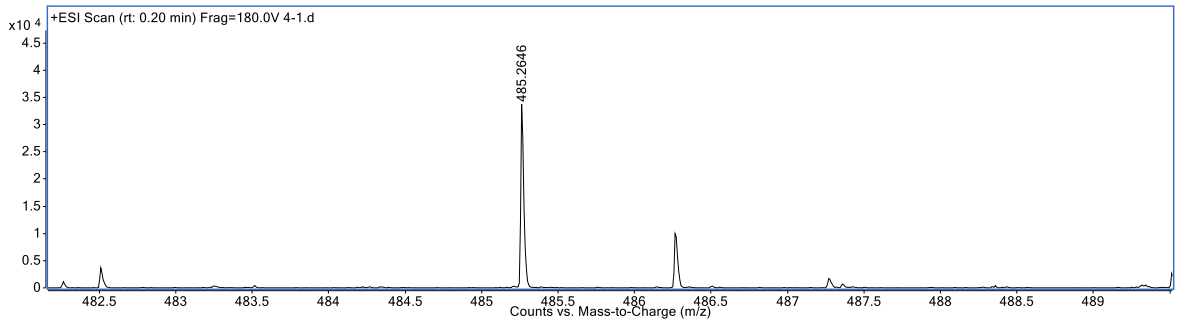

Supplementary Figure 9. High-resolution mass spectrum of conglobatin B2.

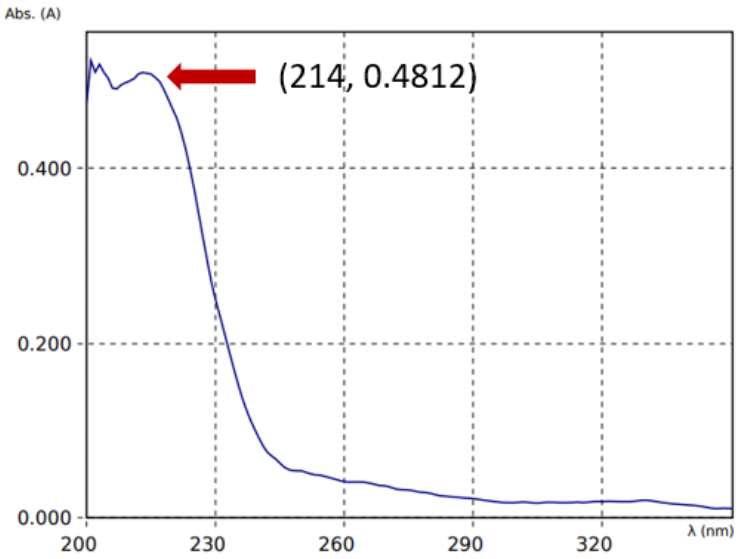

Supplementary Figure 10. UV spectrum of conglobatin B2.

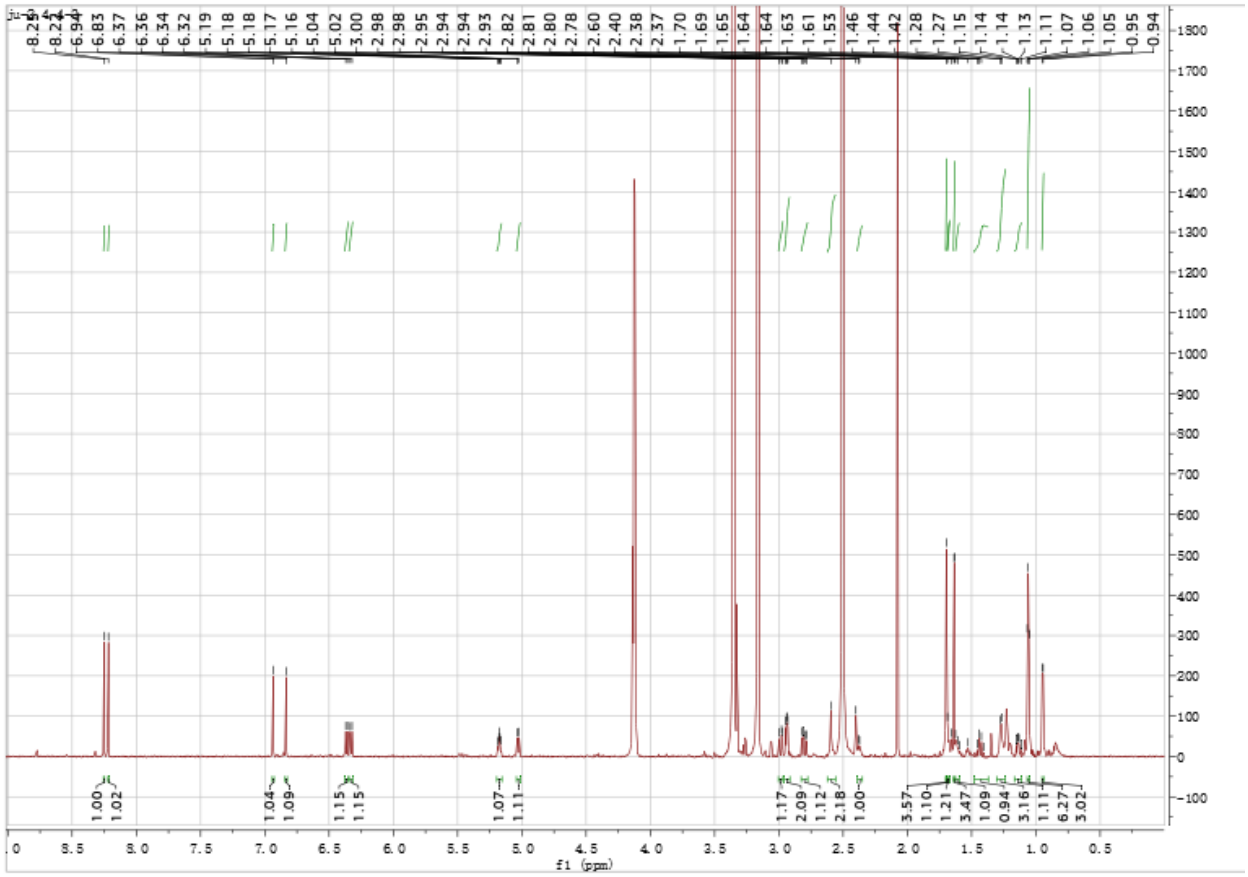

Supplementary Figure 11. ^{1}H NMR spectrum of conglobatin B3 (700 MHz in DMSO-d6).

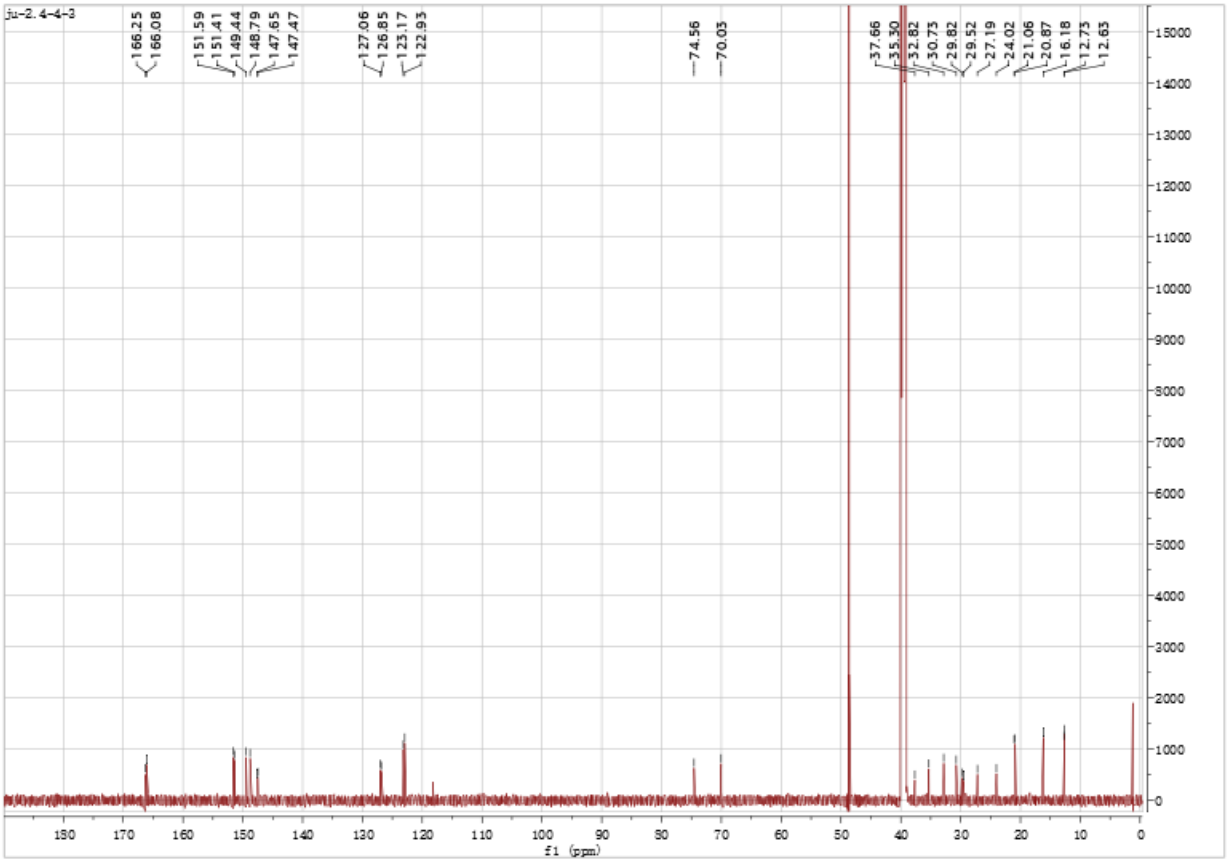

Supplementary Figure 12. ^{13}C NMR spectrum of conglobatin B3 (175 MHz in DMSO-d6).

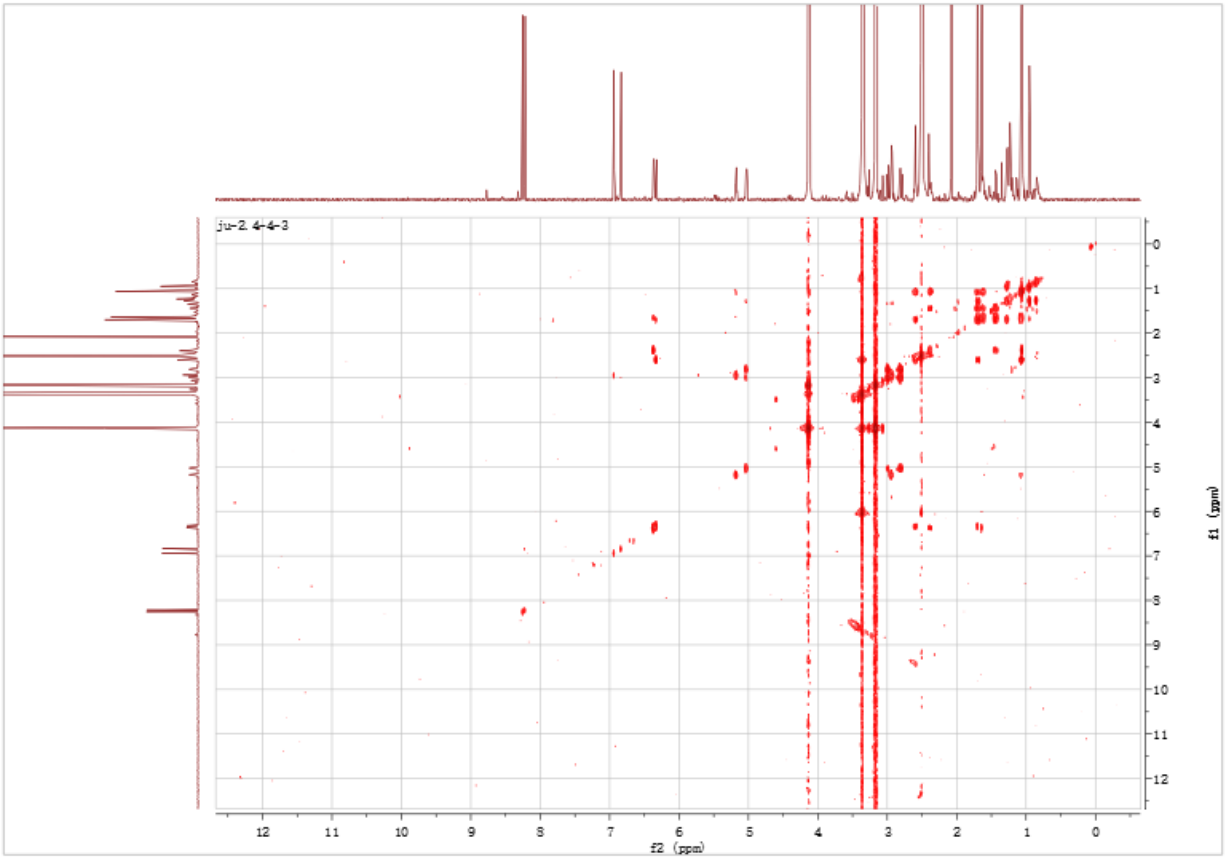

Supplementary Figure 13. ^{1}H-^{1}H COSY spectrum of conglobatin B3 (700 MHz in DMSO-d6).

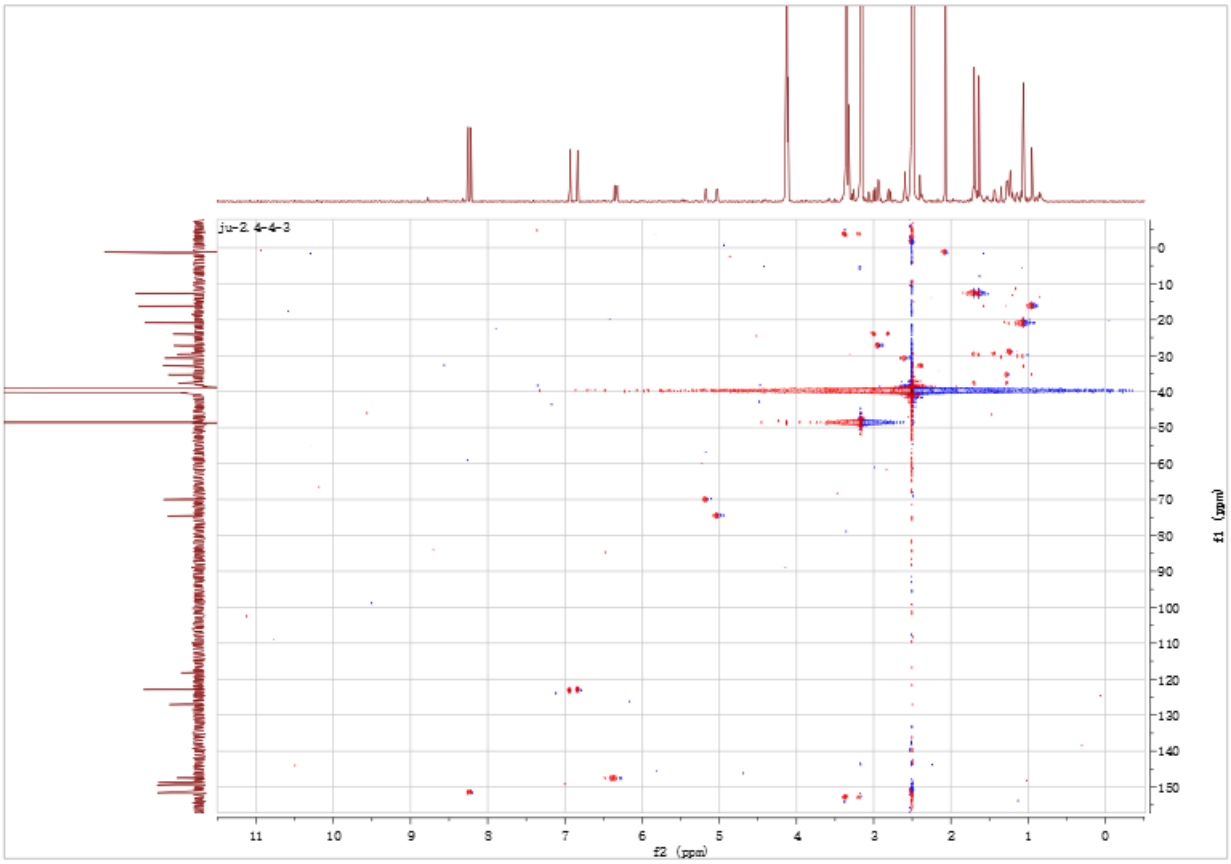

Supplementary Figure 14. HSQC spectrum of conglobatin B3 (700 MHz in DMSO-d6).

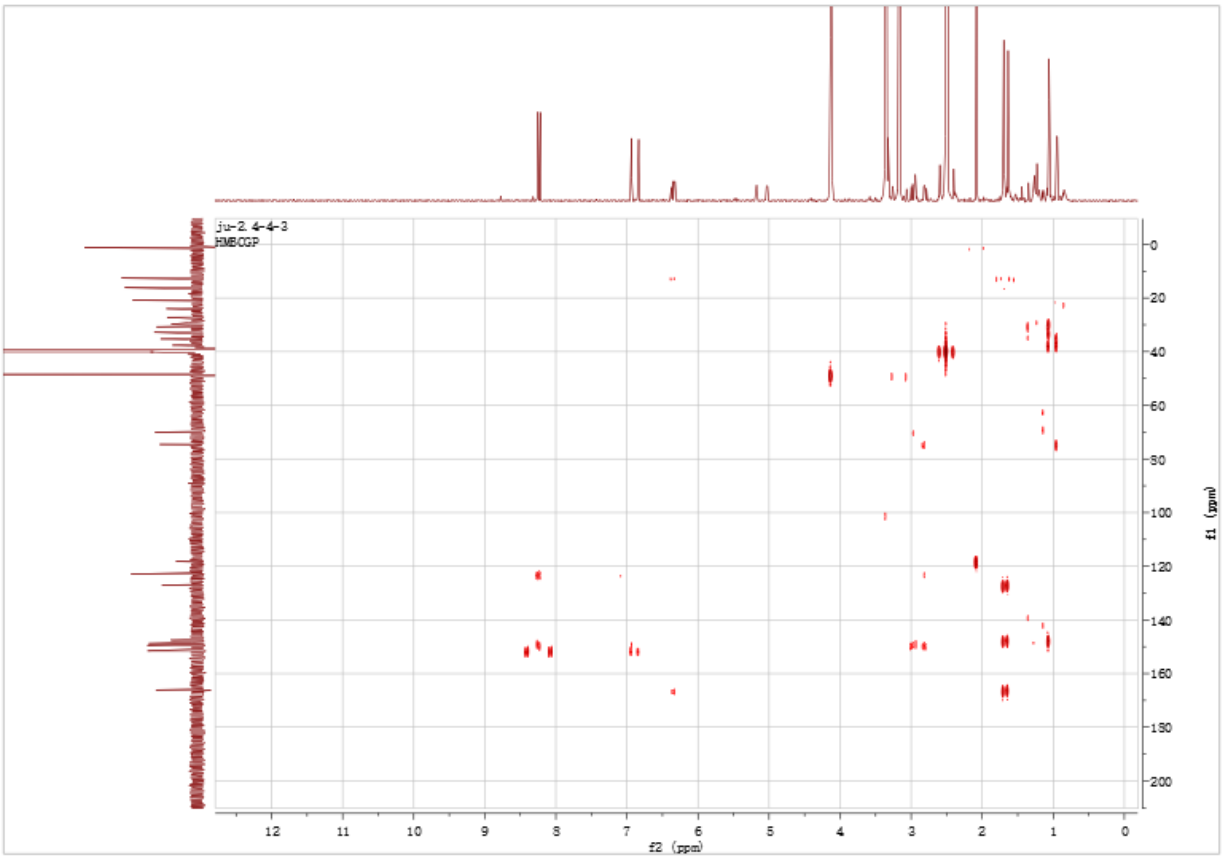

Supplementary Figure 15. HMBC spectrum of conglobatin B3 (700 MHz in DMSO-d6).

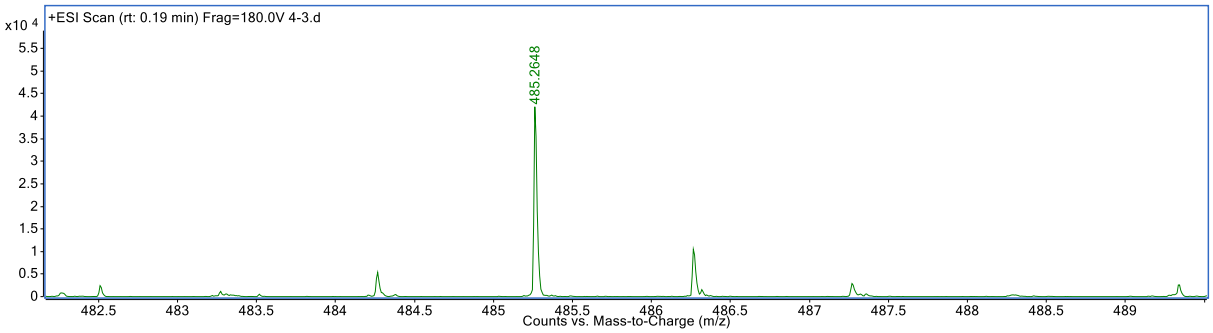

Supplementary Figure 16. High-resolution mass spectrum of conglobatin B3.

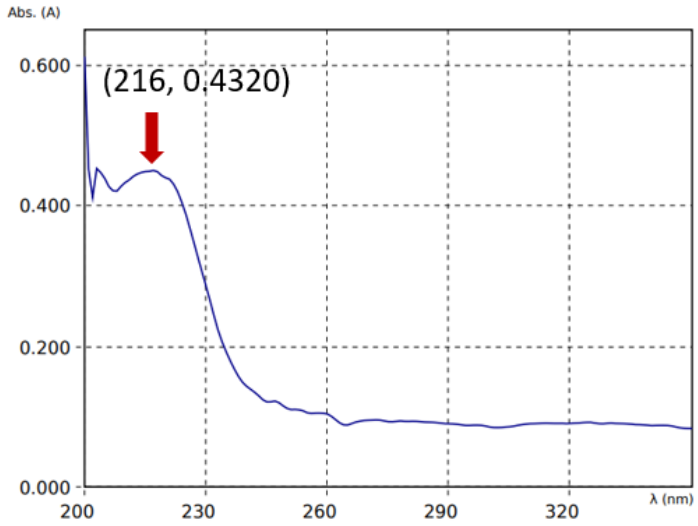

Supplementary Figure 17. UV spectrum of conglobatin B3.

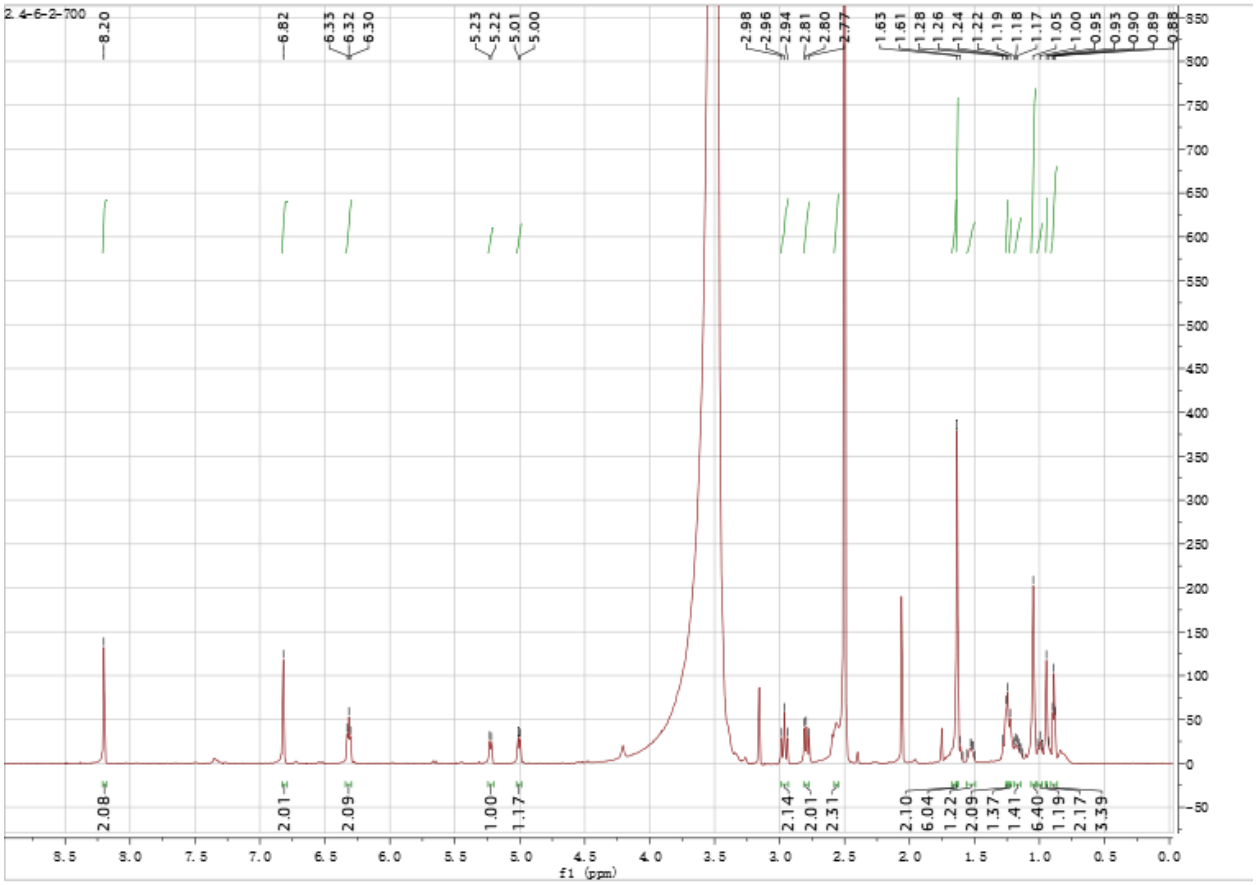

Supplementary Figure 18. ^{1}H NMR spectrum of conglobatin F1 (700 MHz in DMSO-d6).

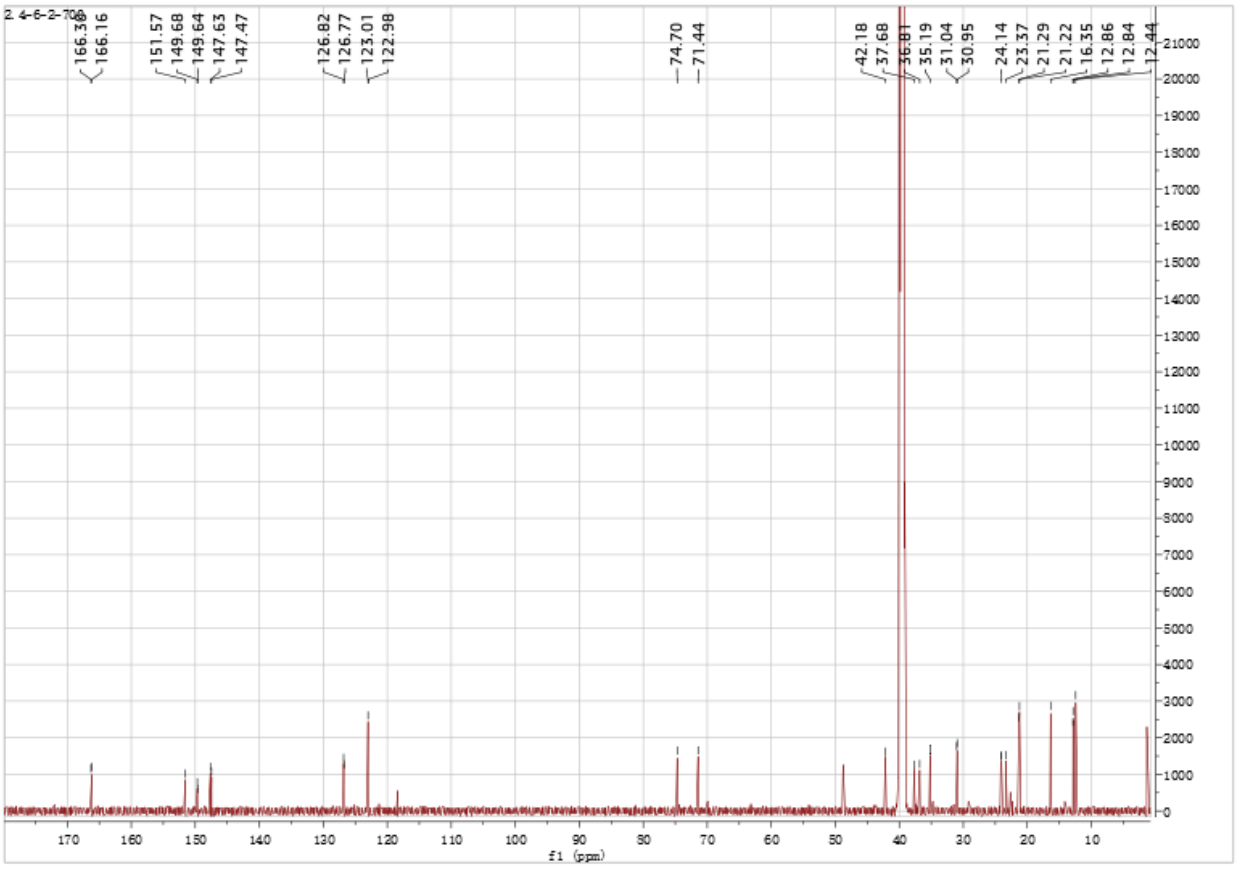

Supplementary Figure 19. ^{13}C NMR spectrum of conglobatin F1 (175 MHz in DMSO-d6).

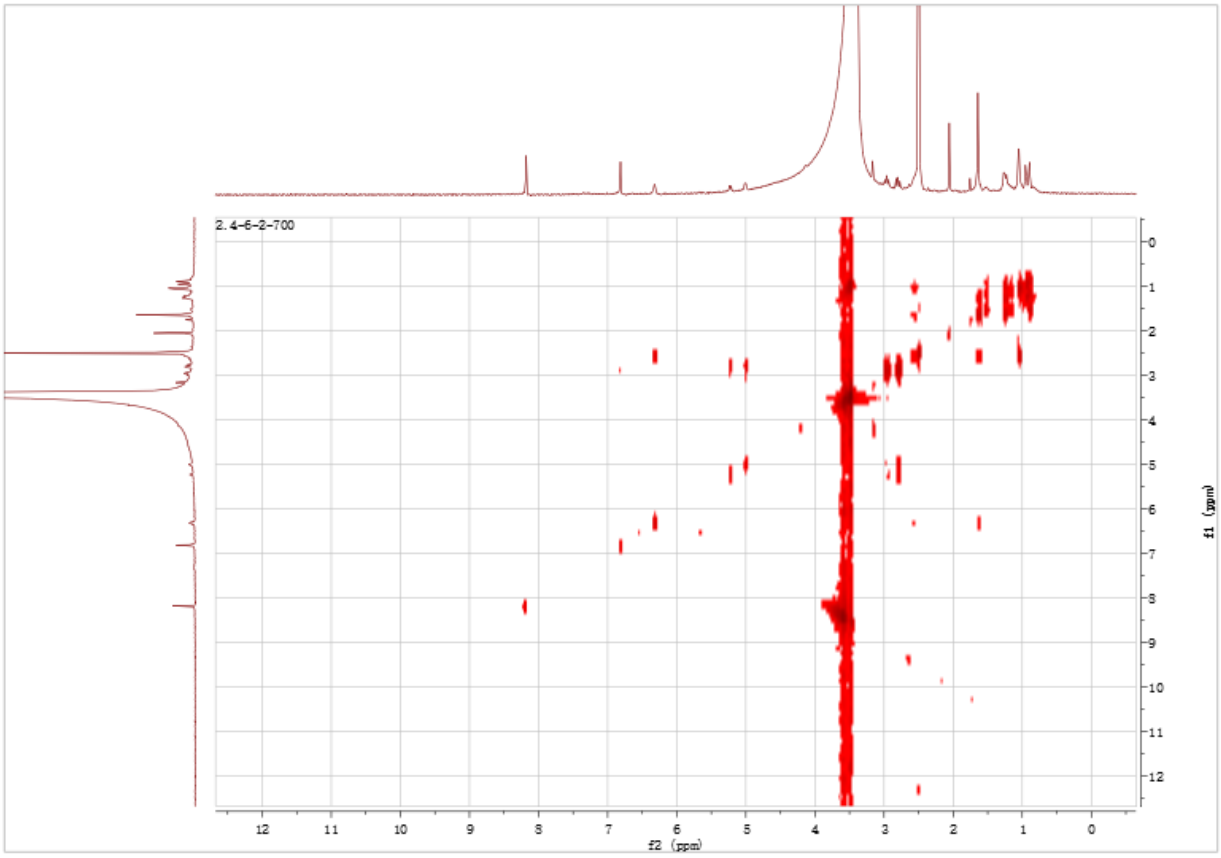

Supplementary Figure 20. ^{1}H-^{1}H COSY spectrum of conglobatin F1 (700 MHz in DMSO-d6).

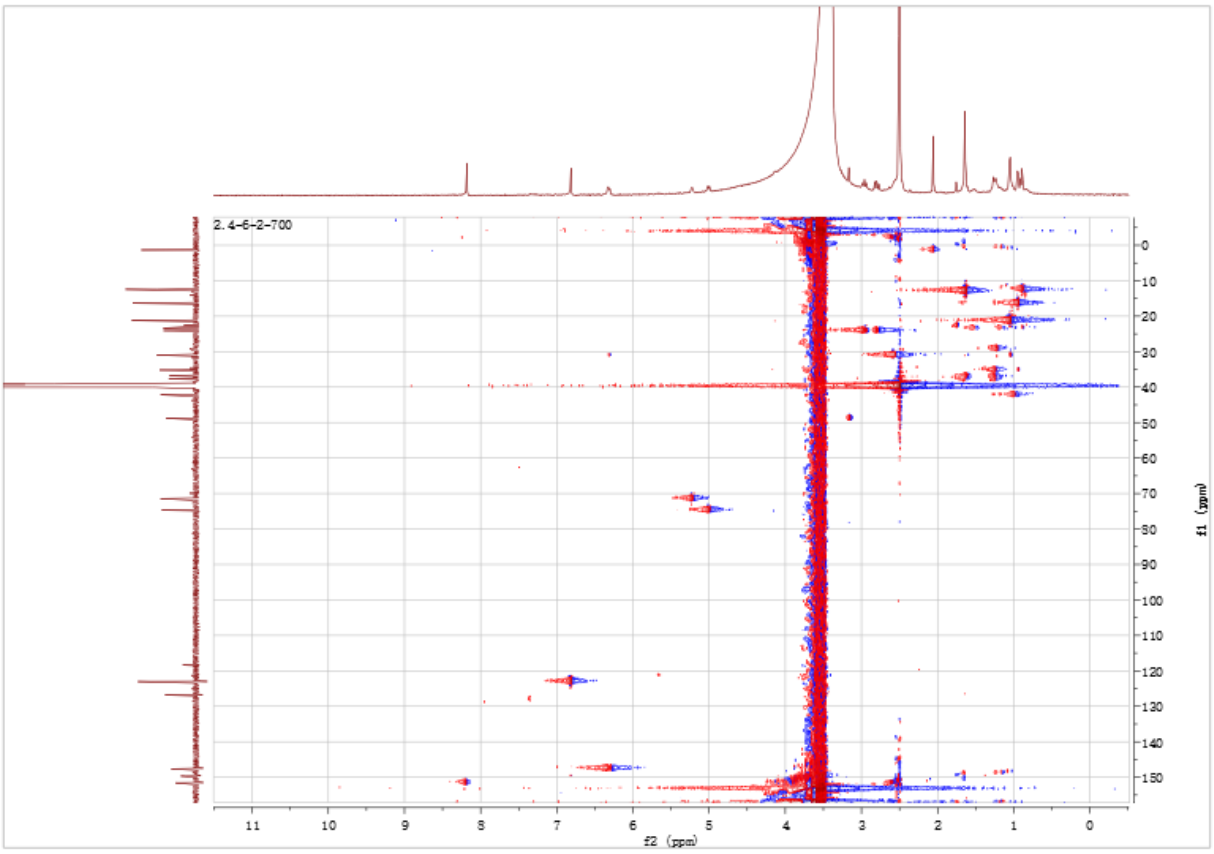

Supplementary Figure 21. HSQC spectrum of conglobatin F1 (700 MHz in DMSO-d6).

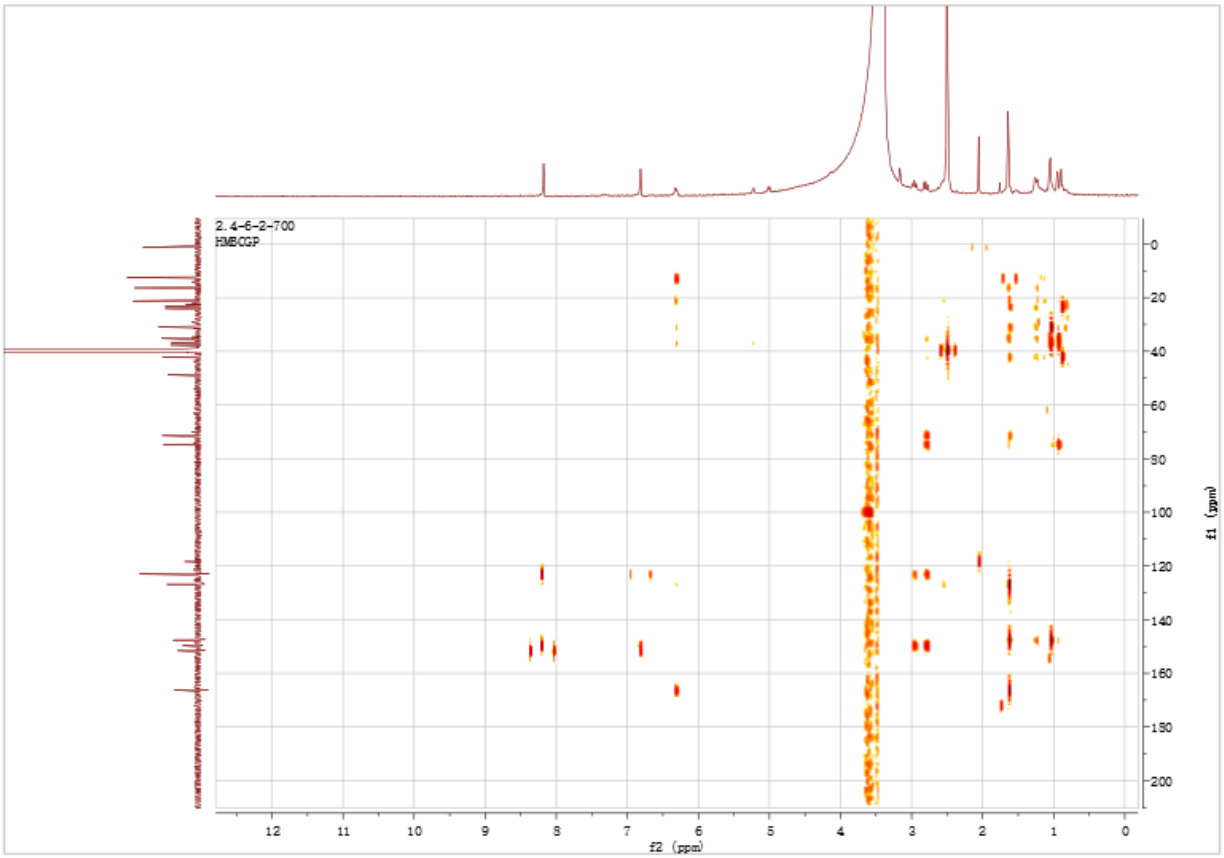

Supplementary Figure 22. HMBC spectrum of conglobatin F1 (700 MHz in DMSO-d6).

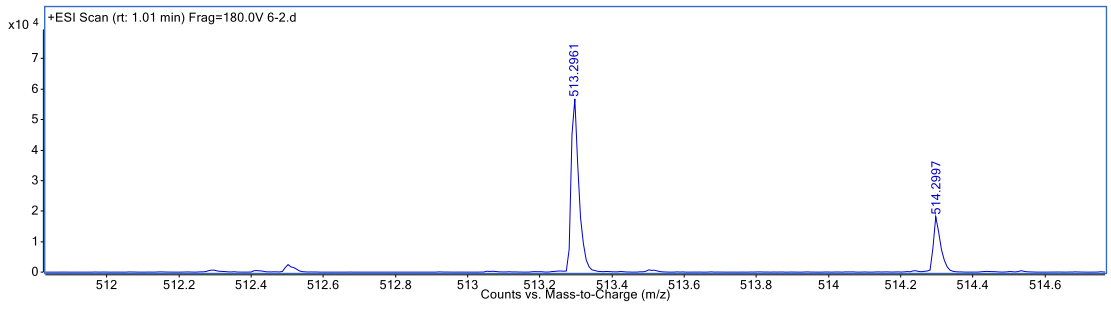

Supplementary Figure 23. High-resolution mass spectrum of conglobatin F1.

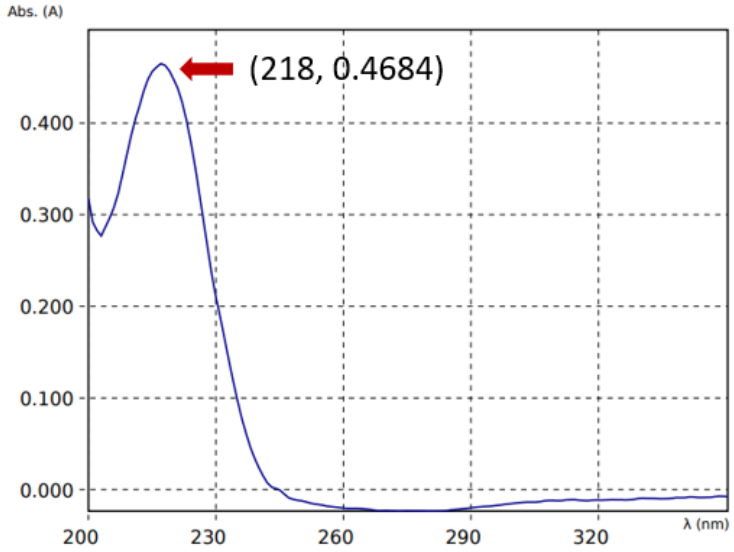

Supplementary Figure 24. UV spectrum of conglobatin F1.

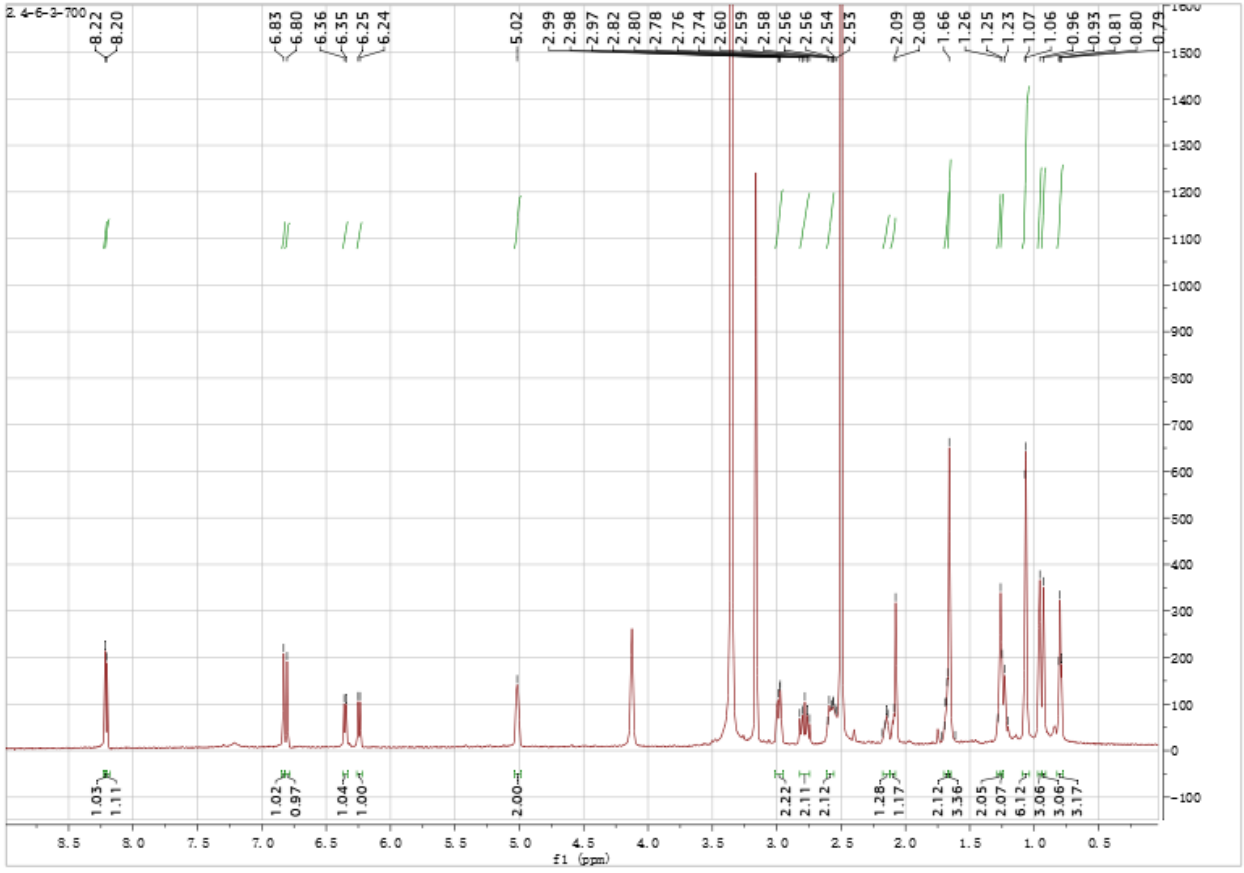

Supplementary Figure 25. ^{1}H NMR spectrum of conglobatin F2 (700 MHz in DMSO-d6).

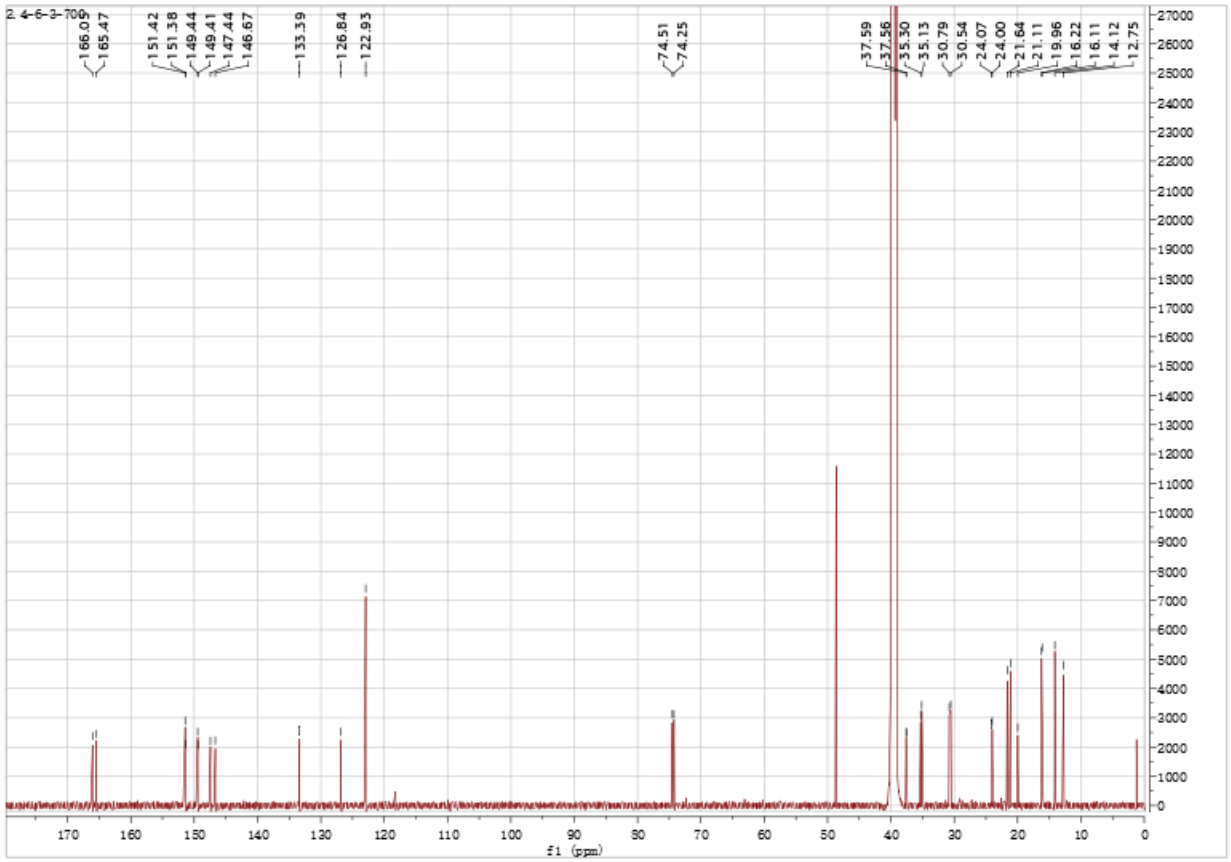

Supplementary Figure 26. ^{13}C NMR spectrum of conglobatin F2 (175 MHz in DMSO-d6).

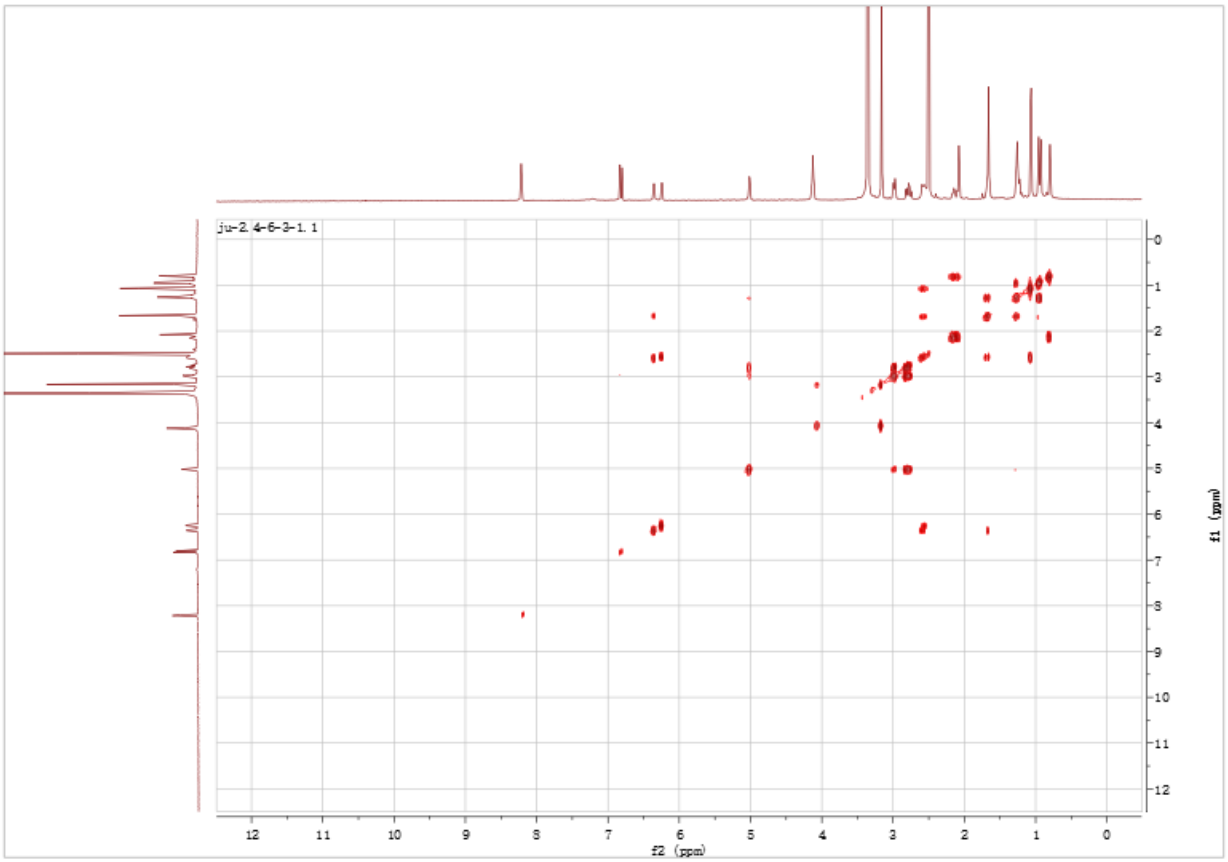

Supplementary Figure 27. ^{1}H-^{1}H COSY spectrum of conglobatin F2 (700 MHz in DMSO-d6).

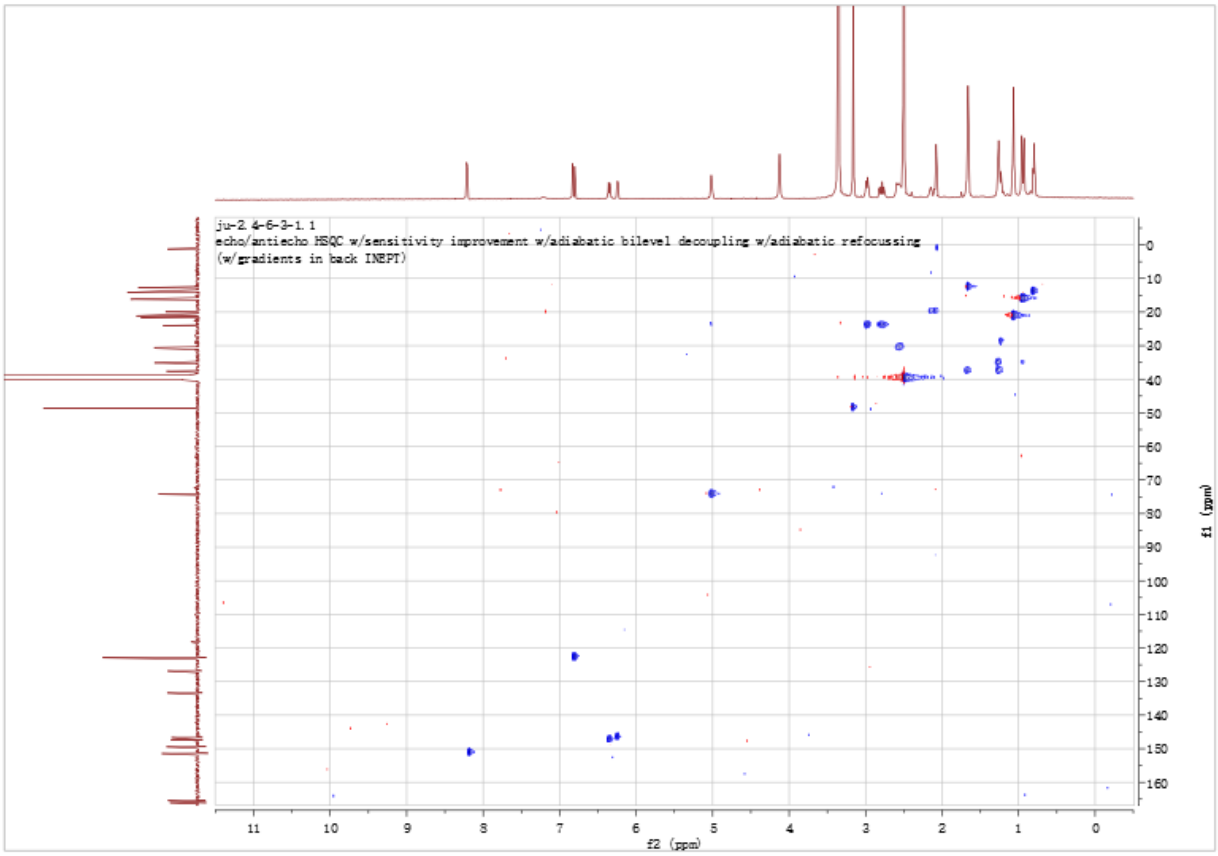

Supplementary Figure 28. HSQC spectrum of conglobatin F2 (700 MHz in DMSO-d6).

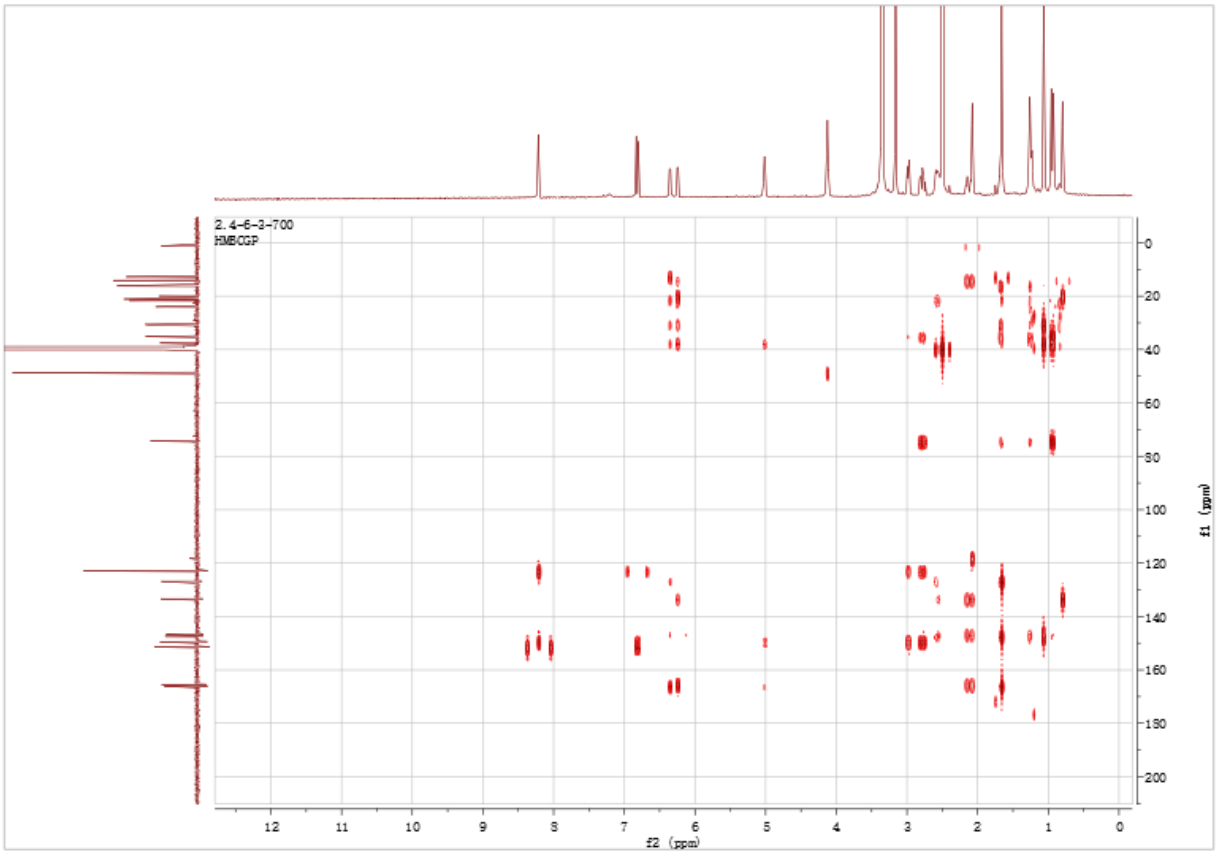

Supplementary Figure 29. HMBC spectrum of conglobatin F2 (700 MHz in DMSO-d6).

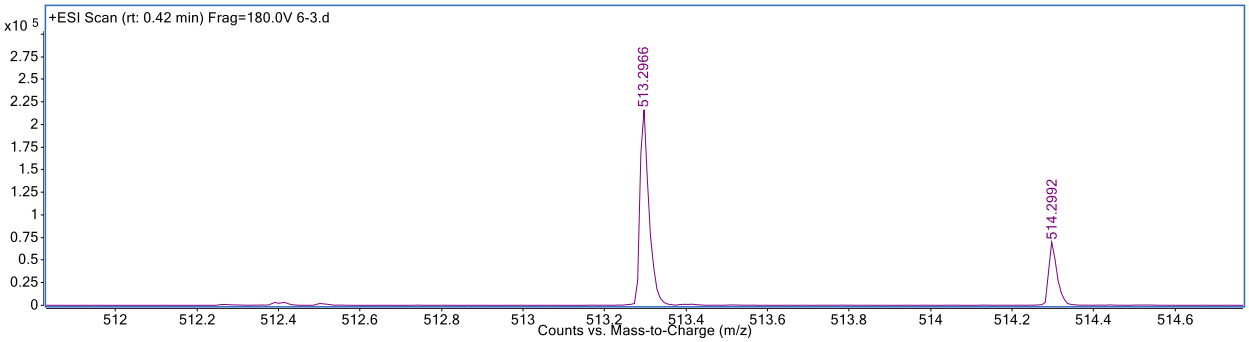

Supplementary Figure 30. High-resolution mass spectrum of conglobatin F2.

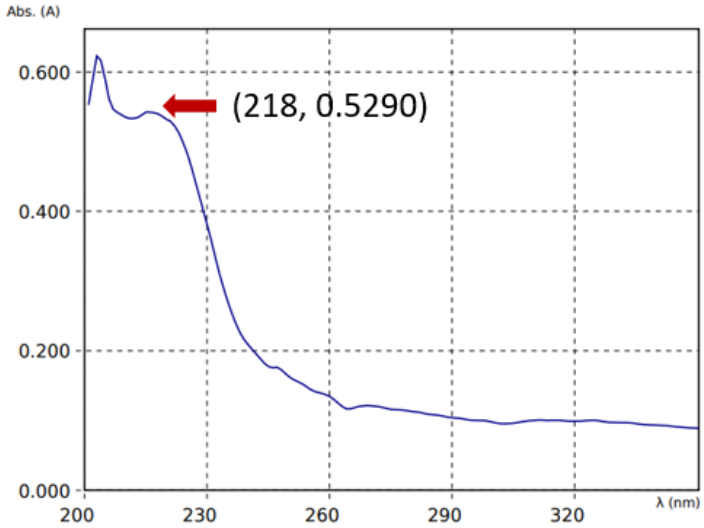

Supplementary Figure 31. UV spectrum of conglobatin F2.

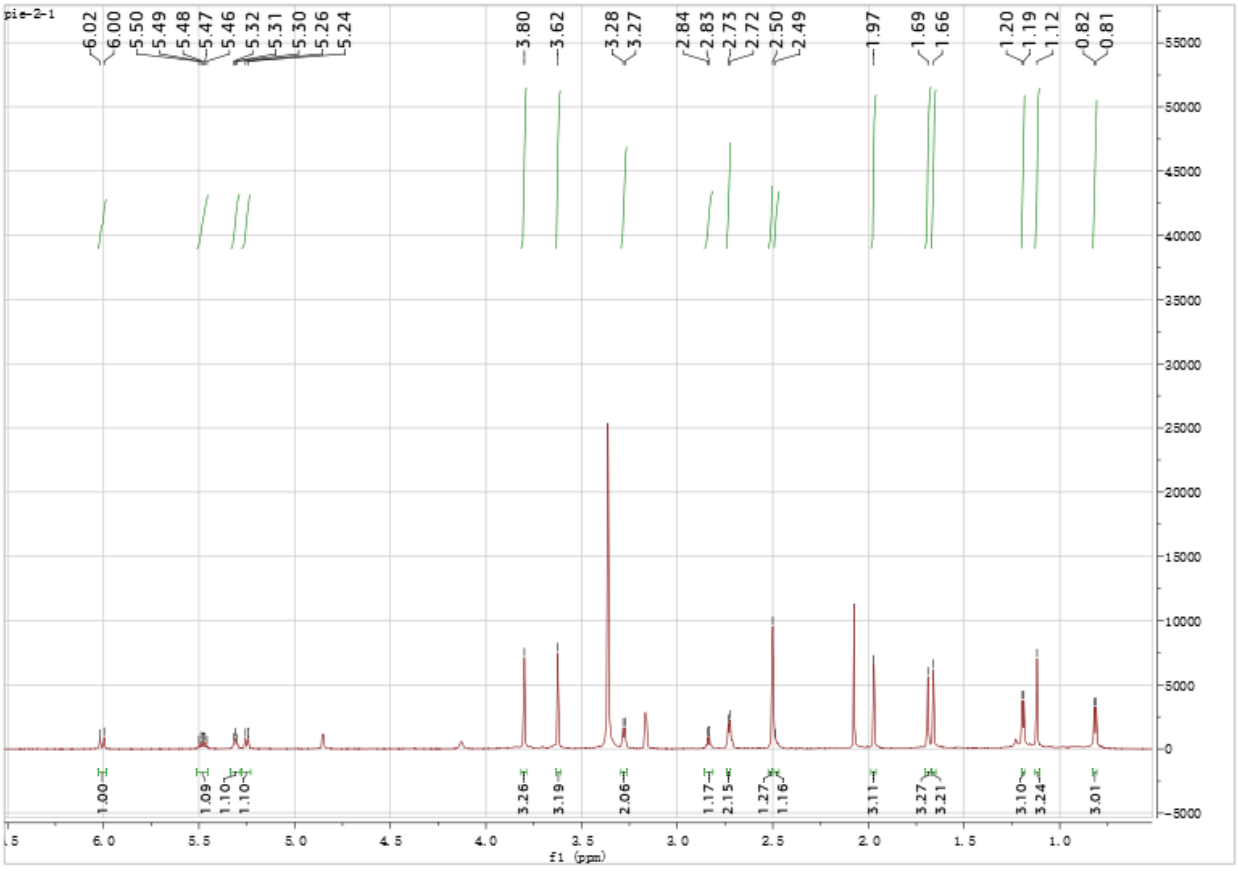

Supplementary Figure 32. ^{1}H NMR spectrum of piericidin C1 (700 MHz in DMSO-d6).

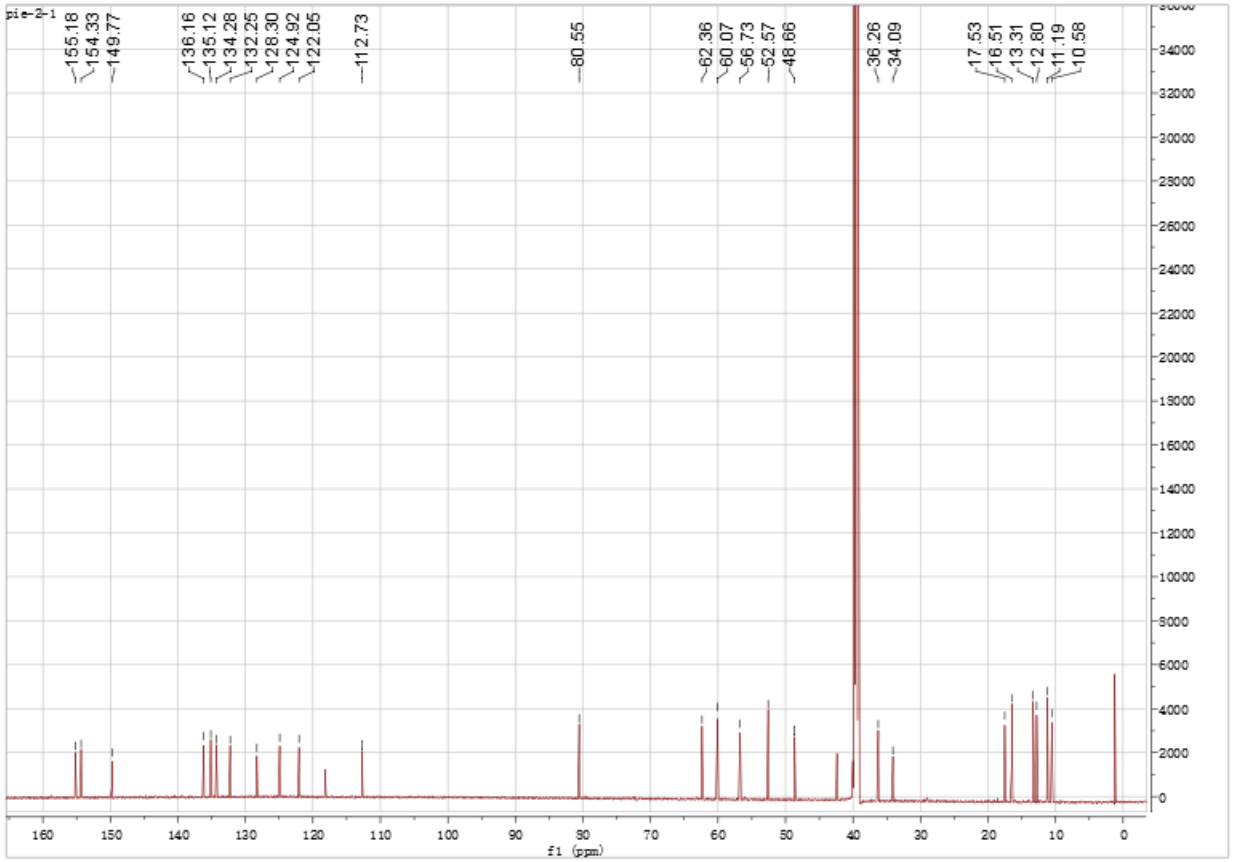

Supplementary Figure 33. ^{13}C NMR spectrum of piericidin C1 (175 MHz in DMSO-d6).

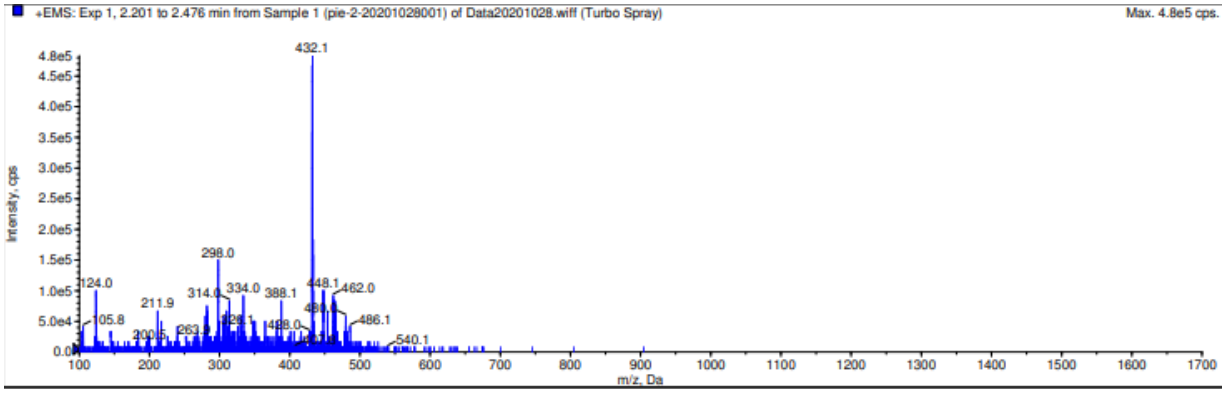

Supplementary Figure 34. Mass spectrum of piericidin C1.

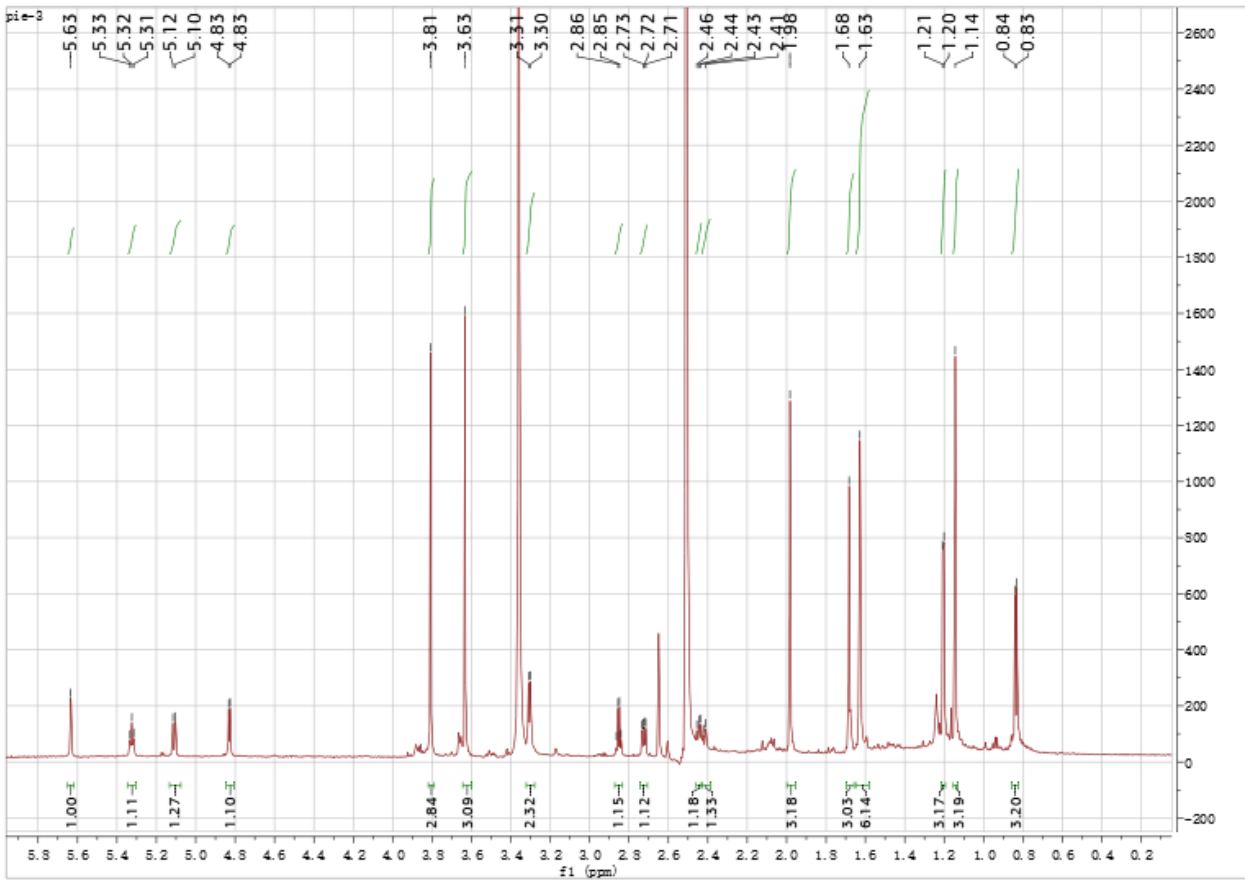

Supplementary Figure 35. ^{1}H NMR spectrum of Mer-A2026A (700 MHz in DMSO-d6).

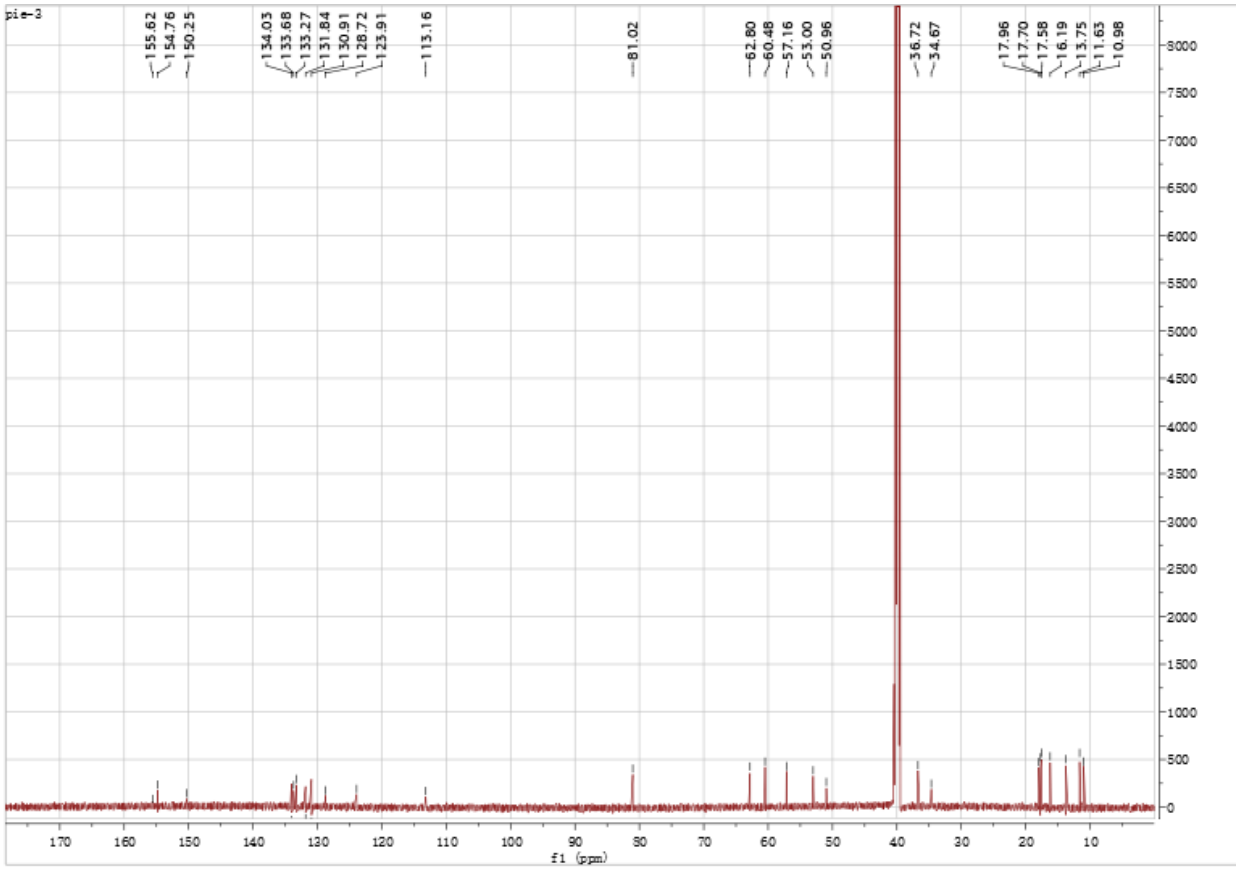

Supplementary Figure 36. ^{13}C NMR spectrum of Mer-A2026A (175 MHz in DMSO-d6).

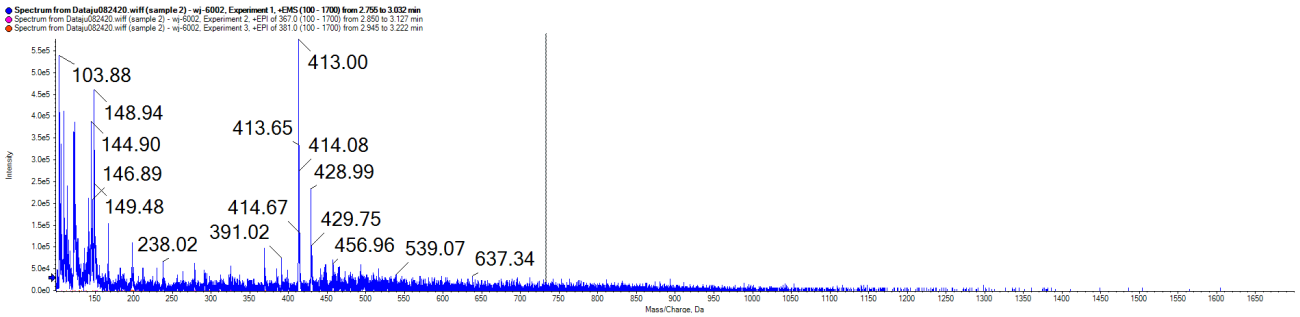

Supplementary Figure 37. Mass spectrum of Mer-A2026A.

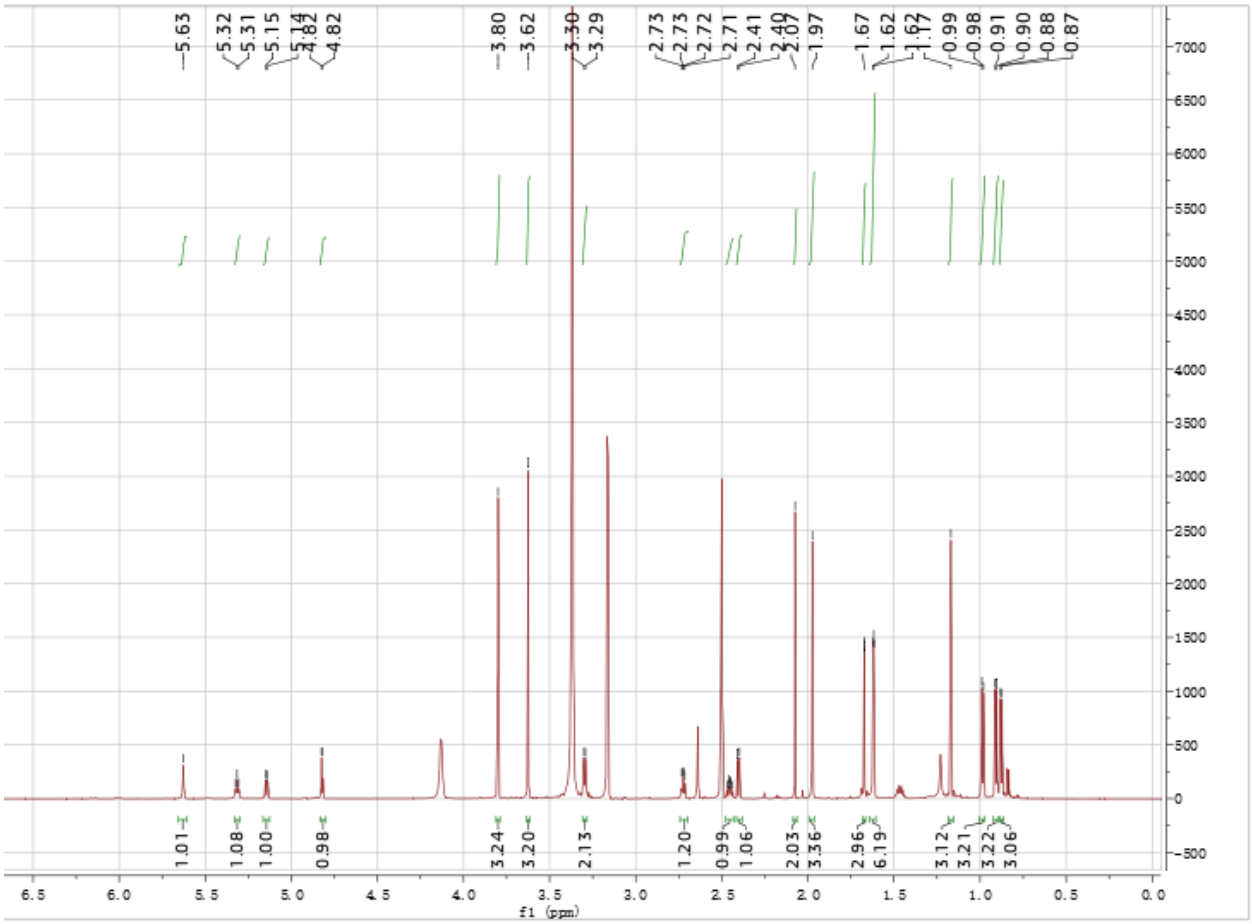

Supplementary Figure 38. ^{1}H NMR spectrum of piericidin C3 (700 MHz in DMSO-d6).

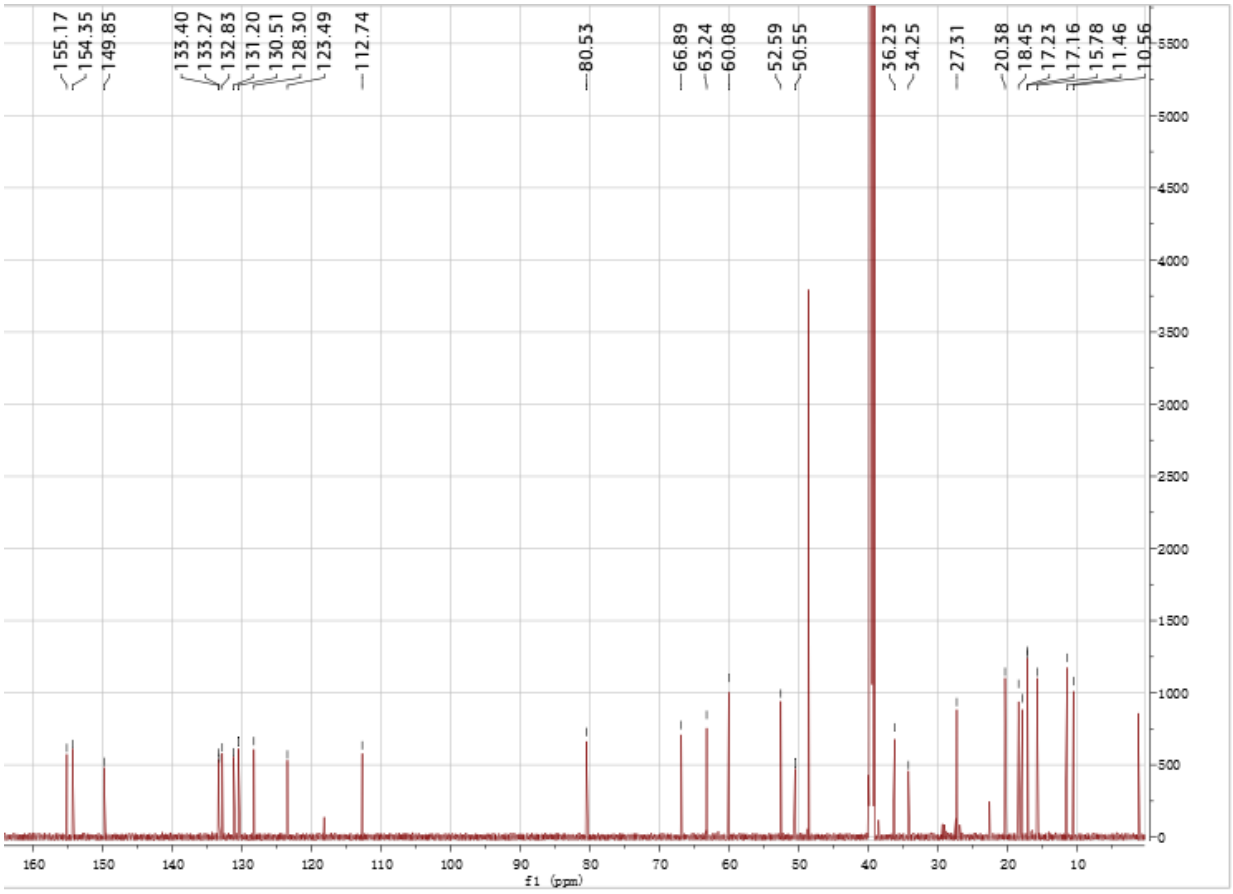

Supplementary Figure 39. ^{13}C NMR spectrum of piericidin C3 (175 MHz in DMSO-d6).

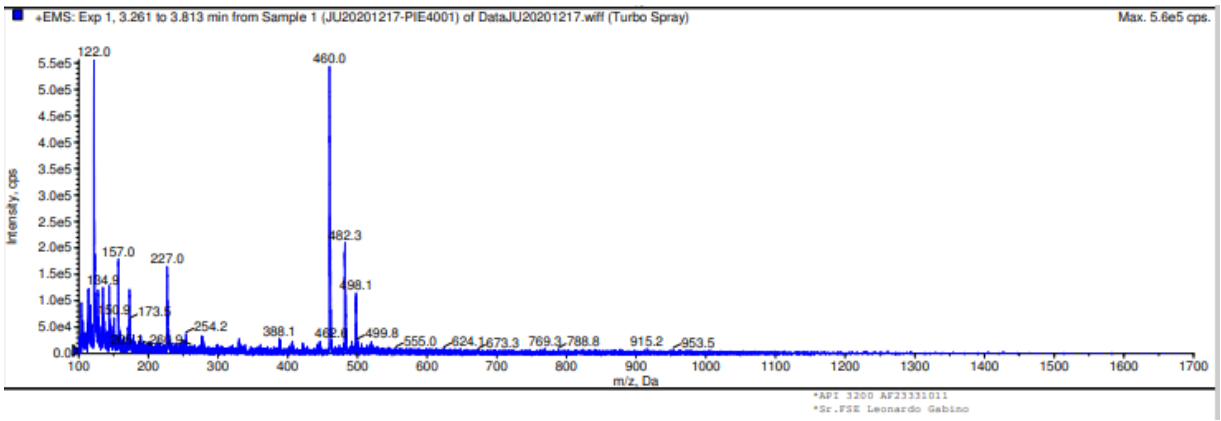

Supplementary Figure 40. Mass spectrum of piericidin C3.

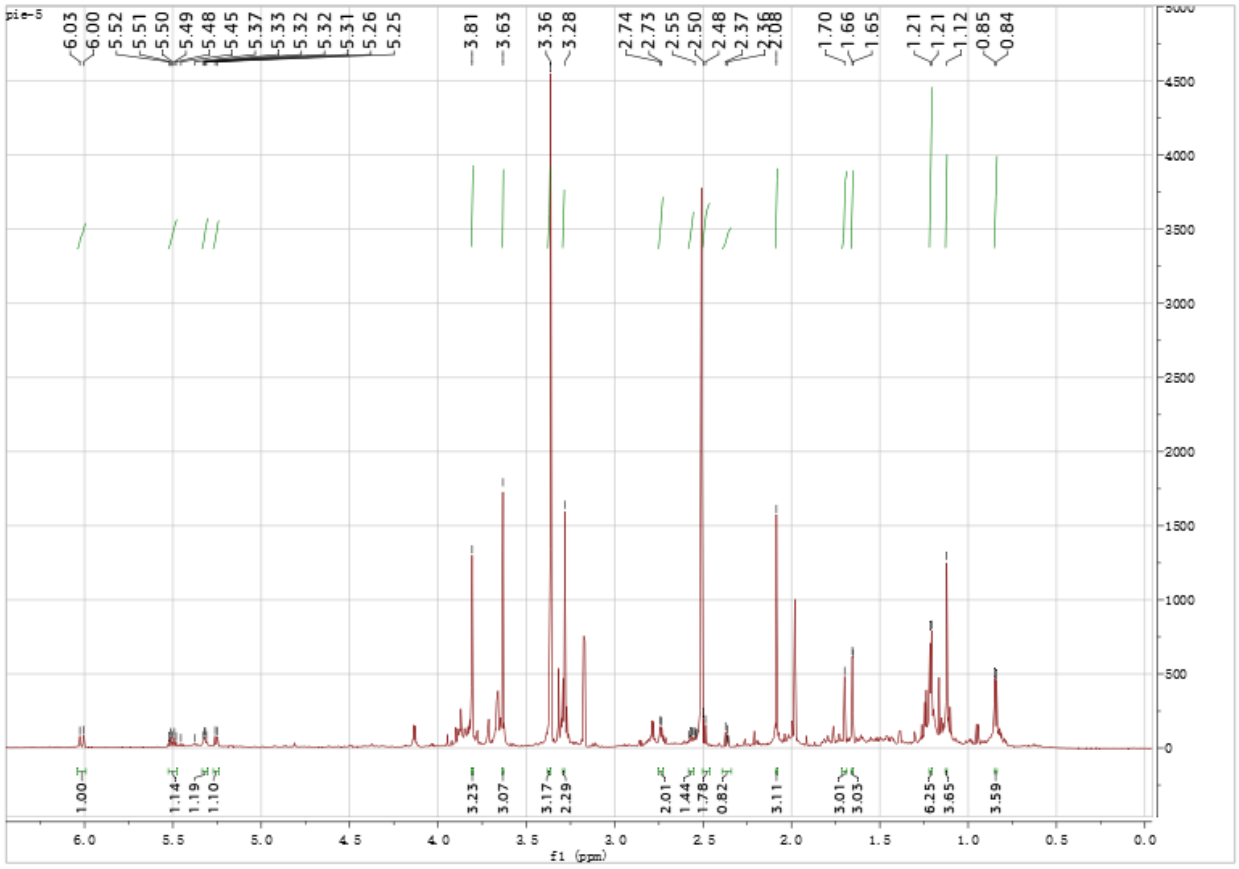

Supplementary Figure 41. ^{1}H NMR spectrum of piericidin D1 (175 MHz in DMSO-d6).

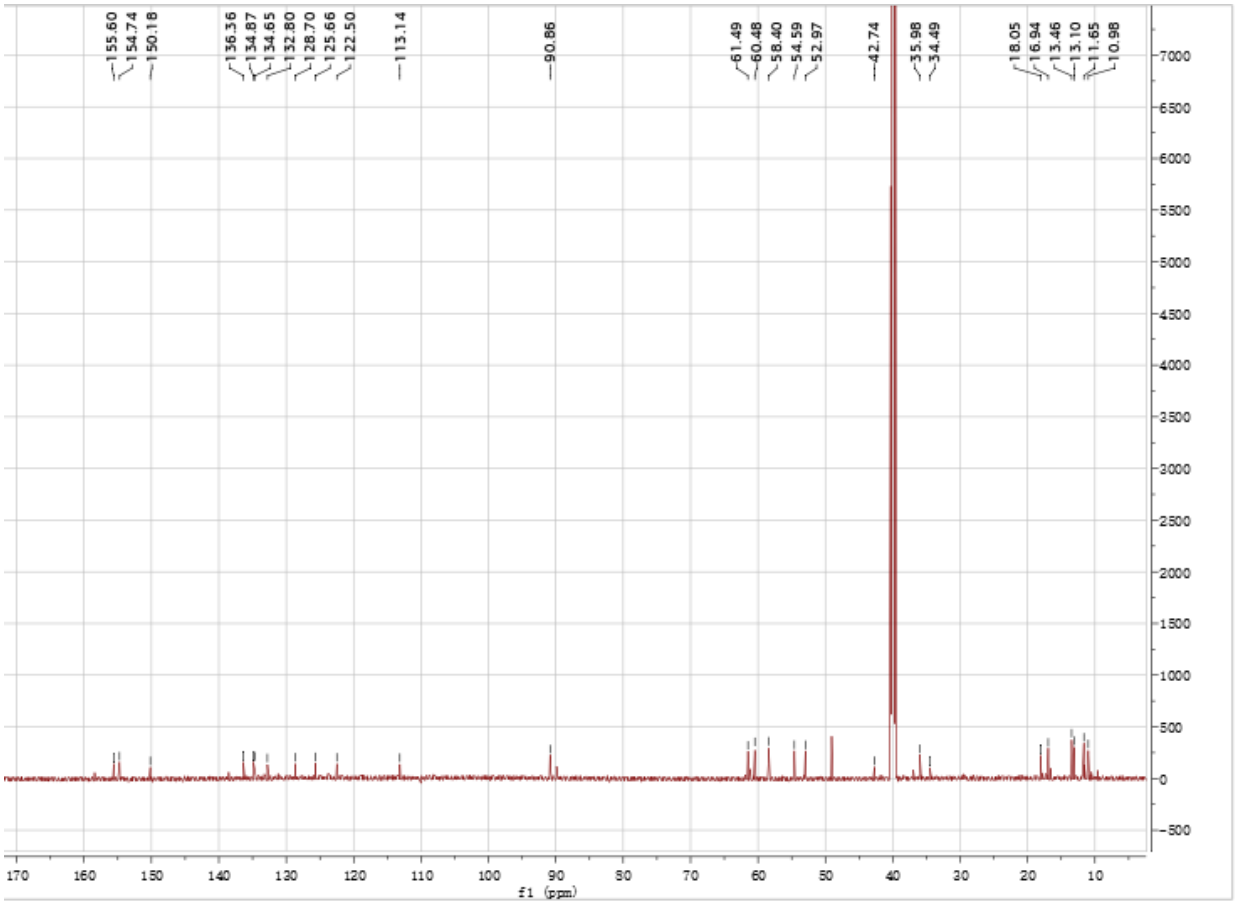

Supplementary Figure 42. ^{13}C-NMR spectra of piericidin D1 (175 MHz in DMSO-d6).

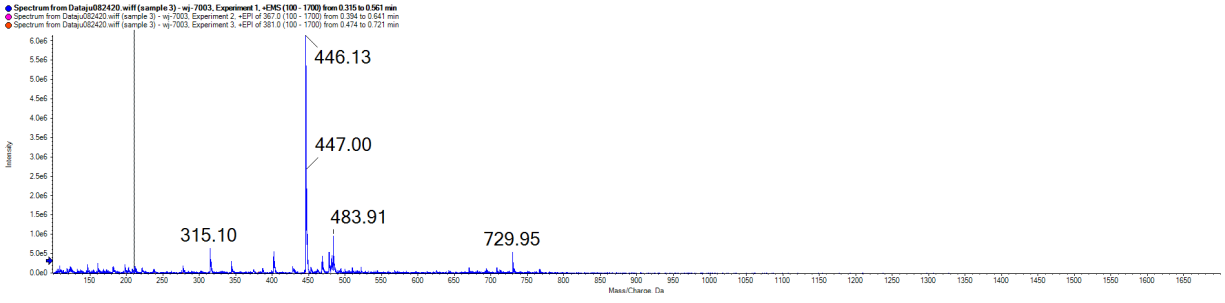

Supplementary Figure 43. Mass spectrum of piericidin D1.

Supplementary References

1. Lu, W., Roongsawang, N., Mahmud, T. (2011) Biosynthetic studies and genetic engineering of pactamycin analogs with improved selectivity toward malarial parasites. *Chem. Biol. 18*, 425-31.
2. Abugrain, M. E., Lu, W., Li, Y., Serrill, J. D., Brumsted, C. J., Osborn, A. R., Alani, A., Ishmael, J. E., Kelly, J. X., Mahmud, T. (2016) Interrogating the tailoring steps of pactamycin biosynthesis and accessing new pactamycin analogues. *ChemBioChem 17*, 1585-8.
3. Zhou, W., Posri, P., Mahmud, T. (2021) Natural occurrence of hybrid polyketides from two distinct biosynthetic pathways in *Streptomyces pactum*. *ACS Chem. Biol. 16*, 270-276.
4. Zhou, W., Posri, P., Abugrain, M. E., Weisberg, A. J., Chang, J. H., Mahmud, T. (2020) Biosynthesis of the nuclear factor of activated T cells inhibitor NFAT-133 in *Streptomyces pactum*. *ACS Chem. Biol. 15*, 3217-3226.